AN ABSTRACT OF THE THESIS OF

Alan Herbert George for the degree of Doctor of Philosophy

in Mechanical Engineering presented on June 4, 1981

Title: An Experimental Study of Heat Transfer to a Horizontal Tube in a Large Particle Fluidized Bed at Elevated Temperature

Redacted for privacy

Abstract approved: James R. Welty

Experimental data for the time-average local heat transfer coefficient, to a single horizontal tube in a large particle fluidized bed at elevated temperature, are presented. An instrumented tube of 50.8 mm diameter, employing the commercially available Micro-Foil Heat Flow Sensor with surface temperature thermocouple, was used. Heat transfer measurements with excellent repeatability were made with the device.

Refractory particles with surface mean diameter 2.14 mm and 3.23 mm were fluidized by combustion products of propane at bed temperatures of 810 K and 1053 K. The particle sizes are near the largest presently used in pilot plant fluidized bed coal combustors. The superficial gas velocity ranged from that required for minimum fluidization, or slightly packed, to the velocity where slugging first occurred, or the highest velocity air blower capacity would allow.

Heat transfer results indicate that a stack of defluidized

particles remain on top of the tube at low superficial gas velocities. A very low local heat transfer coefficient was obtained under these conditions. There was less than 10% difference in the maximum spatial-average heat transfer coefficients for the two particle sizes considered. The maximum spatial-average heat transfer coefficients were approximately 260 $W/m^2 \cdot K$ and 370 $W/m^2 \cdot K$ at bed temperatures of 810 K and 1053 K, respectively.

Available heat transfer results, in the literature, were inadequate to either validate or invalidate the data presented.

An Experimental Study of Heat Transfer to a Horizontal Tube in a Large Particle Fluidized Bed at Elevated Temperature

by

Alan Herbert George

A THESIS

submitted to

Oregon State University

in partial fulfillment of
the requirements for the
degree of

Doctor of Philosophy

Completed May 15, 1981

Commencement June 1982

APPROVED:

Redacted for privacy

Professor of Mechanical Engineering
in charge of major

Redacted for privacy

Head of Department of Mechanical Engineering

Redacted for privacy

Dean of Graduate School

Date thesis is presented June 4, 1981

Typed by Donna Lee Norvell-Race for Alan H. George

ACKNOWLEDGEMENT

The work reported herein was sponsored, in part, by the United States Department of Energy under contract number EF-77-S-01-2714. Additional funding was provided by Battelle Northwest Laboratories.

TABLE OF CONTENTS

Chapter Page

LIST OF FIGURES

LIST OF TABLES

NOTATION

Symbol	Description
$Ar = \frac{gd_p^3(\rho_s - \rho_f)}{\rho_f \nu_f^2}$	Archimedes Number
C_1	Specific heat of stainless steel shim stock
d_p	Surface mean particle diameter
g	Acceleration due to gravity
h_1	Local bed-to-tube heat transfer coefficient (for error analysis in Appendix A)
h_2 =	$1/R_{GAGE}$
h_g	Local bed-to-tube heat transfer coefficient due to pure gas convection (bubbles contacting tube)
h_{Tg}	Local bed-to-tube heat transfer coefficient due to pure gas convection (bubbles contacting tube) for an isothermal surface
$\bar{h}$	Spatial-average bed-to-tube heat transfer coefficient
$\bar{h}_T$	Spatial-average bed-to-tube heat transfer coefficient for an isothermal surface
$\bar{h}_{MAX}$	Maximum spatial-average bed-to-tube heat transfer coefficient

Symbol	Description
h_Θ	Local bed-to-tube heat transfer coefficient
K_i	Overall voltage gain on data channel i
k_1	Thermal conductivity of stainless steel shim stock
k_f	Thermal conductivity of fluidizing gas at the bed temperature
$\overline{Nu}_{MAX} = \frac{d_p \bar{h}_{MAX}}{k_f}$	Maximum spatial-average Nusselt Number
q_1	Heat flux at top surface (bed side) of stainless steel shim stock
q_2	Heat flux at lower surface (tube side) of stainless steel shim stock
q_Θ	Local bed-to-tube heat flux
R_{GAGE}	Thermal resistance of Micro-Foil Heat Flow Sensor
t	Time
t_c	Time constant
T_B	Temperature of fluidized bed
$T_{w\Theta}$	Local surface temperature
$\bar{T}_w$	Spatial-average surface temperature at locations of heat flux measurements

Symbol	Description
T_w	Temperature of stainless steel shim stock (used in Appendix A and Appendix D)
T_{w2}	Temperature at interface between Micro-Foil Heat Flow Sensor and tube (used in Appendix A and Appendix D)
U	Superficial gas velocity
U_{mf}	Superficial gas velocity at minimum fluidization conditions
V^j_{ti}	Transducer voltage output for data channel i at time j
V^j_{OUTi}	Voltage output on data acquisition system for data channel i at time j
V_{OSi}	Offset voltage on data acquisition system for data channel i
x	Coordinate
y	Coordinate

Greek Symbols	Description
δ_1	Thickness of stainless steel shim stock
Δ ( )	Uncertainty in measurement of the quantity ( )
Θ	Angular position on tube surface
ν_f	Kinematic viscosity of fluidizing gas at the bed temperature
ρ_s	Density of particle

Greek Symbols	Description
ρ_f	Density of fluidizing gas at the bed temperature
ρ_l	Density of stainless steel shim stock

Subscripts	Description
MAX	Maximum value or condition which gives maximum error magnitude
RAN	Random calibration and data acquisition errors

Other Symbols	Description
$\doteq$	Approximately equal to

AN EXPERIMENTAL STUDY OF HEAT TRANSFER TO A HORIZONTAL TUBE IN A LARGE PARTICLE FLUIDIZED BED AT ELEVATED TEMPERATURE

I. INTRODUCTION

1.1 General

It is generally acknowledged that high rates of heat transfer can be obtained for surfaces immersed in fludized beds (Botterill, 1975; Kunii and Levenspiel, 1969; Zabrodsky, 1966; Gelperin and Einstein, 1971). Most applications of fluidization employ rather small particles (d_p < 0.5 mm).

Current interest in large particle fluidized beds stems from the recent development of several new processes. The fluidized combustion of coal, in which crushed coal is burned in a bed of dolomite or limestone particles, is possibly the most important. Some advantages of the process, over conventional pulverized coal firing are: (1) It is not necessary to pulverize the coal; (2) Coal with low ash fusion temperature can be burned since stable fluidized bed combustion can be sustained at temperatures as low as 1030 K; (3) Coal of high sulphur content may be burned since most of the sulphur is adsorbed on the bed particles. Recent studies (The Babcock and Wilcox Co., 1979; Leon et al., 1979; Goblirsch et al., 1980; Skinner, 1971) all report promising results based on pilot plant studies.

Heating of process fluids, for example, crude oil, is being studied by Cherrington et al. (1977) at Exxon Research and Engineering Co. Combustion of radioactive waste material has also been carried out in fluidized beds (Petrie et al., 1968).

In all of the above-mentioned applications, horizontal tube arrays have proven to be a practical configuration for the immersed heat exchanger surface.

1.2 Present Work

The present study considers the time-average local heat transfer[1] on the surface of a single horizontal tube, immersed in a large particle fluidized bed at elevated temperature. Both the thermal stress problem for the tube wall and the analysis of coking of process fluids within the tube require local bed-to-tube heat transfer data.

The geometry considered (single horizontal tube) is not one of great practical interest; tube arrays (bundles) being used in most applications. Rather, the present study is preliminary in nature; a first step before the study of more complex configurations.

Particle sizes used (d_p = 2.14 mm and d_p = 3.23 mm) are close to the maximum sizes used as bed material in pilot plant fluidized bed combustors. The maximum bed temperature, for which data were taken, was 1053 K.

1.3 Mechanisms of Heat Transfer Between Fluidized Beds and Immersed Surfaces

It is usual, for the purposes of analysis, to divide the heat transfer into several additive components (see, for example, Gelperin and Einstein, 1971). Those usually identified are: (1) unsteady conduction into solid particles (particle convection); (2) gas convection due to gas flow between particles; (3) gas convection due to bubbles touching the surface; (4) radiation. Several investigators have indicated that the radiative component is not simply additive to the others, but occurs partially at the expense

---

[1] Since only time-average quantities are reported, the words "time-average" will usually be omitted.

of the gas convective and particle convective mechanisms (Botterill and Sealey, 1970; Botterill, 1975; Basu, 1978; Pikashov et al., 1980).

In the experiment reported here, it was not possible to separately measure the various components of the heat transfer. Therefore, no further comments will be made concerning them.

II. PREVIOUS WORK

Results of previous experimental measurements of bed-to-tube heat transfer coefficients, for horizontal tubes in large particle (d_p > 1 mm) gas fluidized beds, are reviewed. Instrumentation used by previous investigators is also briefly discussed.

Reviews of the entire field of fluidized bed heat transfer are available (e.g., Gelperin and Einstein, 1971; Botterill, 1975; Zabrodsky, 1966; and Saxena et al., 1978). No adequate study of the time-average local heat transfer, to a single horizontal tube, in a large particle fluidized bed at elevated temperature, has been reported in the literature.

2.1 Instrumentation

2.1.1 Time-Average Local Measurements

Most studies have employed heat flux measuring elements suitable for use only in low temperature beds. Usually a thin metal foil was attached to the tube surface and heated electrically. The heat transfer rate was computed from the electrical power input. Similar instruments are described by Cherrington et al. (1977), and Chandran et al. (1980).

The instrumented tube used by Chandran et al. (1980) employed electrically heated foils mounted side-by-side around the tube periphery. Since each foil was heated independently, a near isothermal surface temperature was maintained. The other investigators mentioned above used single-position probes, with the heated foil mounted on a tube constructed of insulating material (plexiglas). This design introduces a discontinuity in the surface temperature and requires that the tube be rotated to measure the local heat flux (or local heat transfer coefficient) for all positions of interest.

Berg and Baskakov (1974) obtained local bed-to-tube heat transfer coefficients by measuring the local surface temperature and solving the heat conduction equation for the tube wall. Their technique is of interest, since it is adaptable to use in high temperature beds and does not introduce a temperature discontinuity on the tube's surface.

Samson (1973) deduced the local bed-to-tube heat transfer coefficient by measuring the temperature difference across a bronze plug which was insulated from the tube wall. He noted the difficulty of measuring the small temperature differences involved and other flaws in the technique.

2.1.2 Instantaneous Local Measurements

Thin, electrically heated foils or metallic films of low heat capacity were described by Baskakov et al. (1973a,b), Bernis et al. (1977a,b) and Fitzgerald et al. (1981). None is suitable for use in high temperature fluidized beds.

A circular foil heat flux gage, also called a Gardon gage or asymptotic calorimeter (see Gardon, 1953; 1960), was adapted to use in fluidized beds by Gosmeyer (1979)

2.2 Data and Correlations

2.2.1 Time-Average Local Measurements

Chandran et al. (1980) measured the local heat transfer coefficient on a horizontal tube in a large particle (d_p = 1.58 mm) pressurized (up to 405 kPa) fluidized bed. They found that the heat transfer coefficient, for the largest particle size considered (d_p = 1.58 mm), nearly doubled as the pressure was increased from 101 to 405 kPa.

Local heat transfer measurements were also made by Cherrington

et al. (1977). They performed tests with particles up to 2.5 mm mean size and tubes up to 150 mm diameter.

Both of the above studies used air, at near room temperature, as a fluidizing gas.

2.2.2 Instantaneous Local Measurements

Catipovic (1979) and Catipovic et al. (1978) reported instantaneous local heat transfer coefficients for a horizontal tube. Their results covered a rather wide range of particle sizes ($0.37 \leqslant d_p \leqslant 6.6$ mm). Local voidage data were also reported. Air, at near room temperature, was used as a fluidizing gas.

Baskakov et al. (1973a) also made measurements of local instantaneous heat transfer coefficients for a horizontal tube. They found that emulsion residence time varied at different locations around the perimeter of the tube. Small particles ($d_p = 0.25$ mm) and low bed temperatures were used.

Data were also reported by Gosmeyer (1979) for a mean particle size of 3.21 mm and a bed temperature of approximately 1090 K. His results displayed rather poor repeatability. However, they are the only instantaneous data for fluidized beds operating at elevated temperatures.

2.2.3 Spatial-Average Heat Transfer Coefficient

Data for the spatial-average heat transfer coefficient, in high temperature beds of large particles, were obtained by Wright et al. (1970), for a horizontal tube bundle in a fluidized bed coal combustor. Under similar conditions, Wright et al. (1969) reported the spatial-average heat flux to a horizontal tube bundle.

Other studies of heat transfer in fluidized bed coal combustors were performed by The Babcock and Wilcox Co. (1979), Goblirsch et al. (1980), and Leon et al. (1979). The data of Leon et al.

showed that a tube located near the top surface of the bed had a significantly higher heat transfer coefficient than one near the bottom. Differences of as much as 53% (based on the lower coefficient) were found.

Tang and Howe (1980) also found the heat transfer coefficient to be higher for tubes located relatively high in the bed.

Correlations for the maximum spatial-average Nusselt number ($\overline{Nu}_{MAX}$), as a function of Archimedes number (Ar), have been suggested by Baskakov et al. (1973a,b) and Zabrodsky et al. (1974). These correlations are compared with the results of the present study in Chapter IV.

III. EXPERIMENTAL APPARATUS

Equipment used to measure the local heat transfer rate and local temperature on the surface of a 50.8 mm O.D. tube is described. Also, the Oregon State University High Temperature Fluidized Bed Facility and associated data acquisition equipment are described in this chapter.

3.1 Instrumented Tube for the Measurement of Local Heat Transfer Rate and Surface Temperature

3.1.1 Design Considerations

After survey of the relevant literature on heat flux measurement and errors incurred in heat flux measurement (Brown et al., 1961; ASTM, 1978; Bachman et al., 1965; Westkaemper, 1961; Hornbaker and Rall, 1964; Hager, 1965; Woodruff et al., 1967; Schulte and Kohl, 1970), the following points were found to be important in the design of the instrumented tube:

a. The tube surface must be smooth. Flow of gas and particles around the tube must be undisturbed by surface protrusions. It is particularly important that the surface be smooth near the locations of the heat flux and surface temperature measurement.

b. In operation, the tube should have a near uniform surface temperature around its periphery. That is, the instrumented tube should provide a thermal boundary condition for the fluidized bed similar to that provided by a relatively thin wall steam generator or process heater tube. Investigators (see Botterill, 1975) generally agree that the local heat transfer coefficient is nonuniform around the periphery of the tube. In order to maintain a near uniform surface temperature, the tube must be of high thermal conductivity material and/or relatively thin

wall thickness. Instruments which grossly violate the uniform surface temperature condition have been used by some investigators, for example, Cherrington et al. (1977). The error incurred is debatable.

c. Even if extremely overheated, the instrumented tube should remain structurally sound. This would provide some protection in case of coolant pump failure or operator error.

d. The instrumented tube should be durable enough to withstand many hours of use in the high temperature fluidized bed environment.

3.1.2 Description of the Instrumented Tube

A device which has most of the desirable qualities mentioned in the above section 3.1.1 is shown in Figure 3.1. The tube itself was machined from thick wall SAE 660 bronze hollow bar stock. This material has a thermal conductivity of approximately 86 W/m • K.

Longitudinal grooves were milled in the tube wall; these were used as channels for the lead wires. Each channel was covered by a mild steel bar stock, which was machined to conform to the tube contour. Two stainless steel bands held the wire channel covers in place.

Two Micro-Foil Heat Flow Sensors,[2,3] with copper-constantan surface temperature thermocouples, were bonded to the tube with high

---

[2]Model number 20455-1, RdF Corp., Hudson, New Hampshire. Maximum operating temperature is 533 K.

[3]It was originally planned to mount seven sensors side-by-side around half of the tube periphery. Long delivery time for the needed sensors eliminated this possibility.

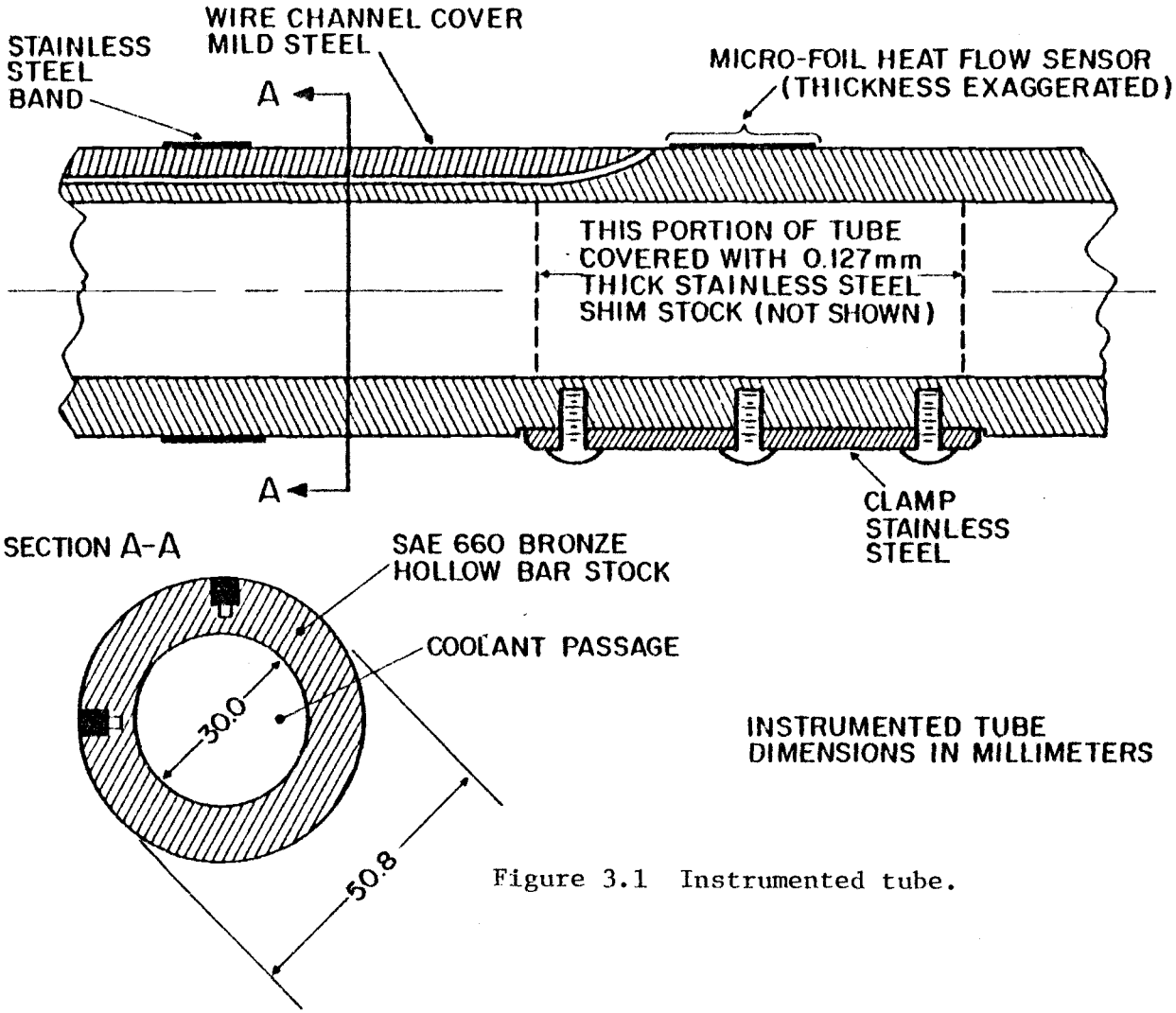

Figure 3.1 Instrumented tube.

temperature thermal conducting epoxy.[4,5] An illustration of the sensor is shown in Figure 3.2. These sensors are less than 0.076 mm thick, except where the lead wires exit the sensors where the thickness is slightly greater. The lead wires were inlaid into the tube wall and ran through the wire channels to the outside. Assembled in this manner, protrusion of the sensor from the tube surface was less than 0.080 mm.

The Micro-Foil Heat Flow Sensor is a thermopile type heat flux transducer. Calibration data, for a particular sensor, are provided by the manufacturer. An early transducer of this type was developed and analyzed by Hager (1965). Others describe similar devices (Brown et al., 1961).

To protect the sensors from the fluidized bed, a 0.127 mm thick stainless steel shim stock, cut to appropriate dimensions, was tightly wrapped around the portion of the tube on which sensors were mounted. This shim stock was held in place by a clamp as shown in Figure 3.1.

To reduce thermal contact resistance, a high thermal conductivity paste[6] was applied under the shim stock, between wire channel covers and wire channels, and under the two stainless steel bands.

3.1.3 Comments on Instrumented Tube Design

The clamp, which holds the shim stock in place, protrudes from

---

[4] Omegabond 200, Omega Engineering, Inc., Stamford, Connecticut.

[5] Due to delays in obtaining the thermal conducting epoxy, one of the sensors was bonded to the tube with M-BOND 610 adhesive from Micro-Measurements, Romulus, Michigan. While performance of this adhesive was satisfactory, the thermal conducting epoxy is to be preferred since it provides a lower contact resistance between the sensor and tube.

[6] Omegatherm 201, Omega Engineering, Inc., Stamford, Connecticut.

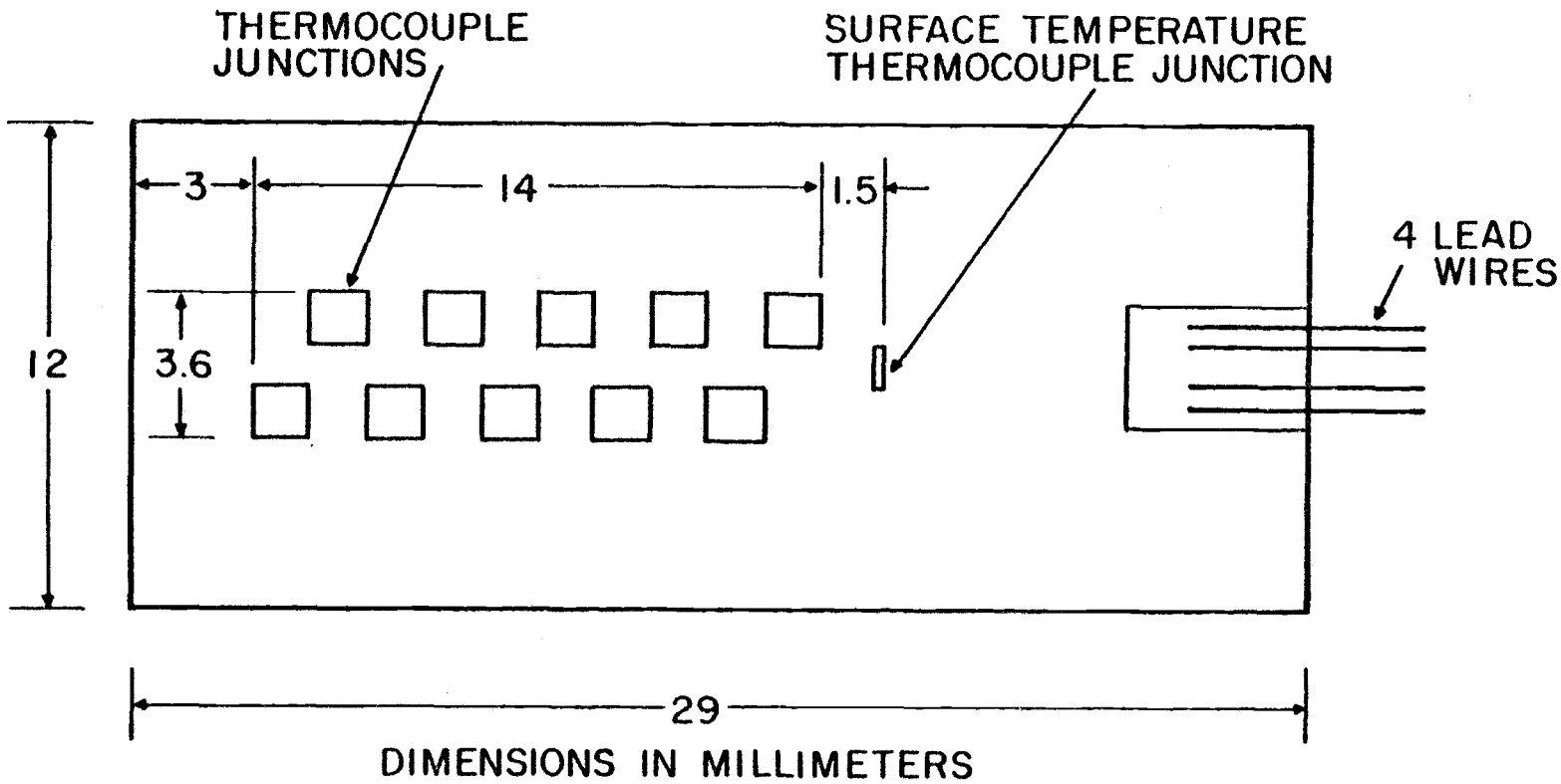

Figure 3.2 Approximate dimensions of the Micro-Foil Heat Flow Sensor. Thickness 0.076 mm.

the tube surface about 3 mm.[7] Air and particle flow around the tube is disturbed by the clamp's presence. However, based on heat transfer results obtained, the error incurred is very small.

A nonuniformity in surface temperature is caused by the presence of the Micro-Foil Heat Flow Sensor. The error in measured heat transfer coefficient is small. A further discussion of this source of error is given in Appendix A (Error Analysis).

For the maximum local heat flux measured during this study, the temperature drop across the stainless steel shim stock was computed to be less than 1.8 K. This was only 0.3% of the bed-to-tube surface temperature difference. The error in surface temperature measurement, due to the presence of the shim stock, was thus negligible and not further considered.

The time constant for the Micro-Foil Sensor and covering shim stock combined, to a step change in surface heat flux, is estimated to be 0.24 seconds (see Appendix D). A time constant of 0.02 seconds is given by the manufacturer, for the Micro-Foil Sensor alone.

3.2 Description of Data Acquisition Equipment

In operation, the Micro-Foil Heat Flow Sensor, with surface temperature thermocouple, produces analog voltages which are directly related to the quantities of principal interest: the local heat flux and local surface temperature. From this information the local heat transfer coefficient was computed.

The analog form of the data was processed to a useful form by the steps shown in Figure 3.3. Equipment used for data acquisition and reduction is described below.

---

[7] A clamp which more closely fits the tube contour could be designed. The present design was used for ease of fabrication.

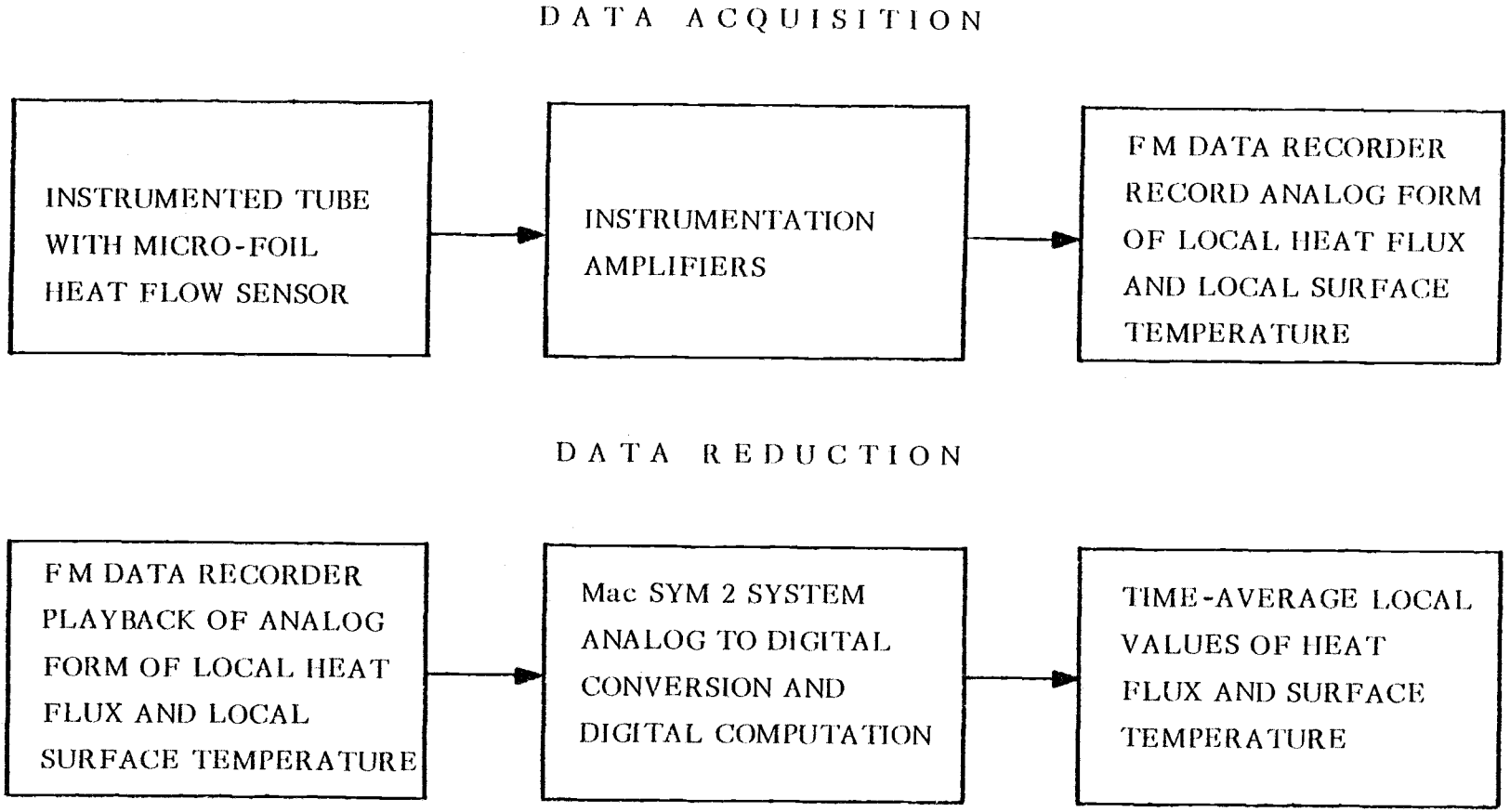

Figure 3.3 Flow diagram of data acquisition and data reduction process.

3.2.1 Instrumentation Amplifiers

A total of four data channels were used during the experiment: two for local heat flux and two for local surface temperature. For each channel, a high quality instrumentation amplifier,[8] with adjustable gain and offset, was provided.

3.2.2 FM Data Recorder

A Lockheed Store 4 FM data recorder was used to store the local heat flux and local surface temperature data in analog form. The recorder was thoroughly checked for operational fitness by the Oregon State University Electronics Service Shop. It was found that a very high quality recording tape[9] was required for the Store 4 to record and playback with good signal quality. Performance of the unit was excellent throughout the study.

3.2.3 MacSym 2 System

The MacSym 2 System[10] provided a 12-bit analog-to-digital converter[11] (accurate to one part in 4096) and digital processing via a MacBasic [12] language compiler. Operation of the system is covered in the reference manuals (Analog Devices, 1980a,b).

---

[8]Model AD522, Analog Devices, Norwood, Massachusetts. The amplifiers were assembled and tested by Gosmeyer (1979).

[9]Scotch Brand "Instrument Tape" and Maxell "UD35-90" both worked well.

[10]Analog Devices, Norwood, Massachusetts.

[11]Model AIM03 analog-to-digital converter, Analog Devices, address as above.

[12]Version of the BASIC computer language with many additional commands.

As presently configured, the system does not have hardcopy capability. Therefore, no listing of the MacBasic program used in the data reduction process is given. The equations used in the data reduction are, however, given in Appendix B (Data Reduction).

3.3 Oregon State University High Temperature Fluidized Bed Facility

A schematic illustration of the Oregon State University High Temperature Fluidized Bed Facility is shown in Figure 3.4. A complete description of the facility, including engineering drawings, is given in Welty (1978). Principal components are described below.

3.3.1 Air Metering System

To measure the air flow rate into the combustion chamber and test section, a ASME standard (ASME, 1959) venturi meter was used. Calibration of the meter was performed by Gosmeyer (1979), who developed a FORTRAN computer program to compute the superficial gas velocity, in the bed, from the venturi pressures and flowing air temperature. The only modification to the program, made during this study, was use of the barometric pressure on the day a given experiment was performed, rather than standard atmospheric pressure.

3.3.2 Propane Burner and Temperature Controller

A proportional type controller was used to regulate the propane flow rate and maintain the desired combustion chamber exit temperature. The combustion chamber is refractory lined. No combustion occurred in the bed itself.

3.3.3 Test Section and Distributor Plate

The refractory lined test section provided mounting ports for

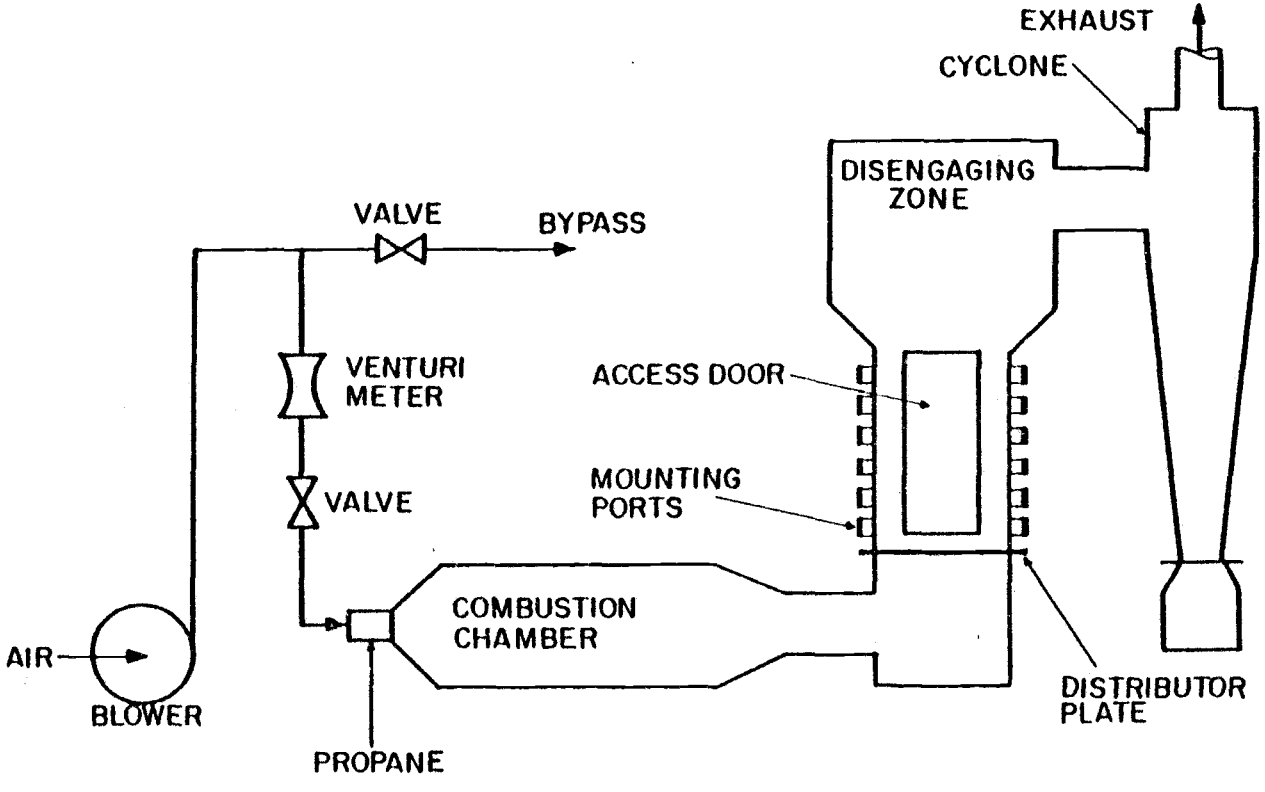

Figure 3.4 Schematic illustration of the Oregon State University High Temperature Fluidized Bed Facility.

the instrumented tube at 0.152 m vertical increments. Cross-sectional dimensions of the fluidized bed are 0.60 x 0.30 m. Pressure taps are provided at 0.102 m vertical increments.

A digital thermometer and chromel-alumel thermocouple (type K) were used to measure the fluidized bed temperature. The thermocouple was located about 0.152 m above the distributor plate and protruded into the fluidized bed about 0.102 m.

A 3.18 mm thick stainless steel (ASTM 310) distributor plate, with 171 holes of 6.35 mm diameter in a square array pattern 31.75 x 31.75 mm, was used. To prevent particle flow back, when the bed was not fluidized, a stainless steel (ASTM 316) 16-mesh screen with 0.457 mm wire diameter was placed under the plate. This screen was supported by a second plate, identical to the first except having 9.53 mm diameter holes.

Operating experience has shown distributor plate life to be acceptable, provided the combustion chamber exit temperature is limited to 1175 K. Failure, due to metal creep, will occur rapidly if this limit is exceeded.

3.3.4 Cooling System for Instrumented Tube

To maintain the instrumented tube at the desired temperature (about 470 K), a light oil (primary coolant), with commercial designation DEXRON II, was pumped through the coolant passage. A shell-and-tube heat exchanger, with water as a secondary coolant, was used to maintain the primary coolant at a reasonable temperature (about 300 K).

IV. EXPERIMENTAL RESULTS

Experimental results for local heat transfer coefficient and spatial-average heat transfer coefficient, to the surface of a 50.8 diameter horizontal tube, immersed in a large particle high temperature fluidized bed, are reported.

Particles of surface mean diameter 2.14 mm and 3.23 mm were fluidized at bed temperatures of 810 K and 1053 K. Documentation of test conditions is also given in this chapter.

4.1 Test Conditions

4.1.1 Bed Material

A granular refractory material with commercial designation Ione Grain A was used for bed material. Chemical composition of this material is given by the supplier[13] as: 53.5% silica, 43.8% alumina, 2.3% titania, 0.4% other. The particles had a smooth surface and fairly spherical shape from several previous test runs.

No reliable data for the thermal conductivity or specific heat of Ione Grain A are known to the writer. However, Chung et al. (1972) and Ziegler et al. (1964) found the thermal conductivity of the particle to be an insignificant factor concerning heat transfer to surfaces immersed in fluidized beds. For large particle beds ($d_p > 1$ mm), Zabrodsky et al. (1978) found no significant dependence on either the thermal conductivity or volumetric heat capacity of the particles. Other properties, directly related to the particles, are summarized in Table 4.1. The surface mean diameter, d_p, shown in Table 4.1, was computed as in Kunii and Levenspiel (1969).

4.1.2 Geometry

Packed bed height was 0.50 m for all cases reported. The

---

[13] Interpace Corporation, Portland, Oregon.

TABLE 4.1 PARTICLE PROPERTIES

density ρ_s = 2700 Kg/m^3

screen analysis:

screen opening mm	mass fraction	mass fraction
Larger	0.0717	0.0016
4.70	0.1217	0.0028
3.99	0.2975	0.0061
3.33	0.4632	0.3648
2.36	0.0377	0.3692
2.00	0.0070	0.1933
1.68	0.0012	0.0466
1.17		
Smaller	0.000	0.0154
d_p =	3.23 mm	2.14 mm

centerline of the instrumented tube was located about 0.31 m above the distributor plate.

Design of the instrumented tube was covered in Chapter III of this document. Design of the Oregon State University High Temperature Fluidized Bed Facility was also given in Chapter III.

4.1.3 Minimum Fluidization Velocity

Fluidized beds of large particles with wide size spectrum, as used here, have no well-defined minimum fluidization velocity (Botterill and Teoman, 1980; Doicher and Akhmakov, 1979; Babu et al.,

1978; Wright et al., 1970). Cherrington et al. (1977) refers to the "nominal minimum fluidization velocity," when working with such systems.

For this study, the superficial gas velocity was reduced, from that required to sustain bubbling, until the pressure drop across the bed started to decrease sharply. This velocity was found to be repeatable within ±10%, and is reported as the minimum fluidization velocity (U_{mf}). Values obtained are shown in Table 4.2.

TABLE 4.2 MINIMUM FLUIDIZATION VELOCITY

T_B K	d_p mm	U_{mf} m/s
810	2.14	1.42
810	3.23	2.07
1052	2.14	1.62
1053	3.23	2.21

The value of U_{mf} plays no direct role in the data reduction or presentation.

4.1.4 Experimental Procedure

The instrumented tube was mounted in the test section, coolant lines attached, and bed filled with particles. The fluidized bed temperature was increased slowly; according to the warm-up schedule given by Welty (1978).

Since only two sensors (heat flux transducers) are mounted on the tube, it was necessary to turn the tube in order to obtain heat

flux and surface temperature data around half the tube periphery. Heat transfer data were taken for five positions, spaced in angular increments of $\pi/4$ radians. Approximately 90 seconds of data were recorded for each condition.

A more detailed experimental procedure, being of use only to those who will conduct future research at the same fluidized bed facility, is given in Appendix C.

4.2 Experimental Results

4.2.1 Heat Transfer Data

Data for the local heat transfer coefficient (h_θ), with d_p = 3.23 mm and T_B = 1053 K, for a range of superficial gas velocities, are shown in Figure 4.1. The excellent agreement between the readings given by sensor 1 and sensor 2, for the $\theta = \pi/2$ radian position, are clearly shown. Good agreement was found for the other cases considered also; the maximum discrepancy was always less than 7%. Typically the difference was even smaller.

Similar plots, to that shown in Figure 4.1, were constructed on fine grid graph paper. This allowed interpolating the data on convenient increments of superficial gas velocity. Figures 4.2, 4.3, 4.4 and 4.5 show the local heat transfer coefficient for both particle sizes and bed temperatures considered in this study. Figure 4.6 shows the spatial-average heat transfer coefficient ($\bar{h}$). This average value was obtained by applying the trapezoidal rule for numerical quadrature (see, for example, Hamming, 1973) to the local values of the heat transfer coefficient.

The velocity range covered is from minimum fluidization, or slightly packed, to the velocity at which slugging first occurred, or the highest which air blower capacity would allow. Bed temperature was controlled to within ±6 K for all cases reported.

Figure 4.7 shows the spatial-average tube surface temperature

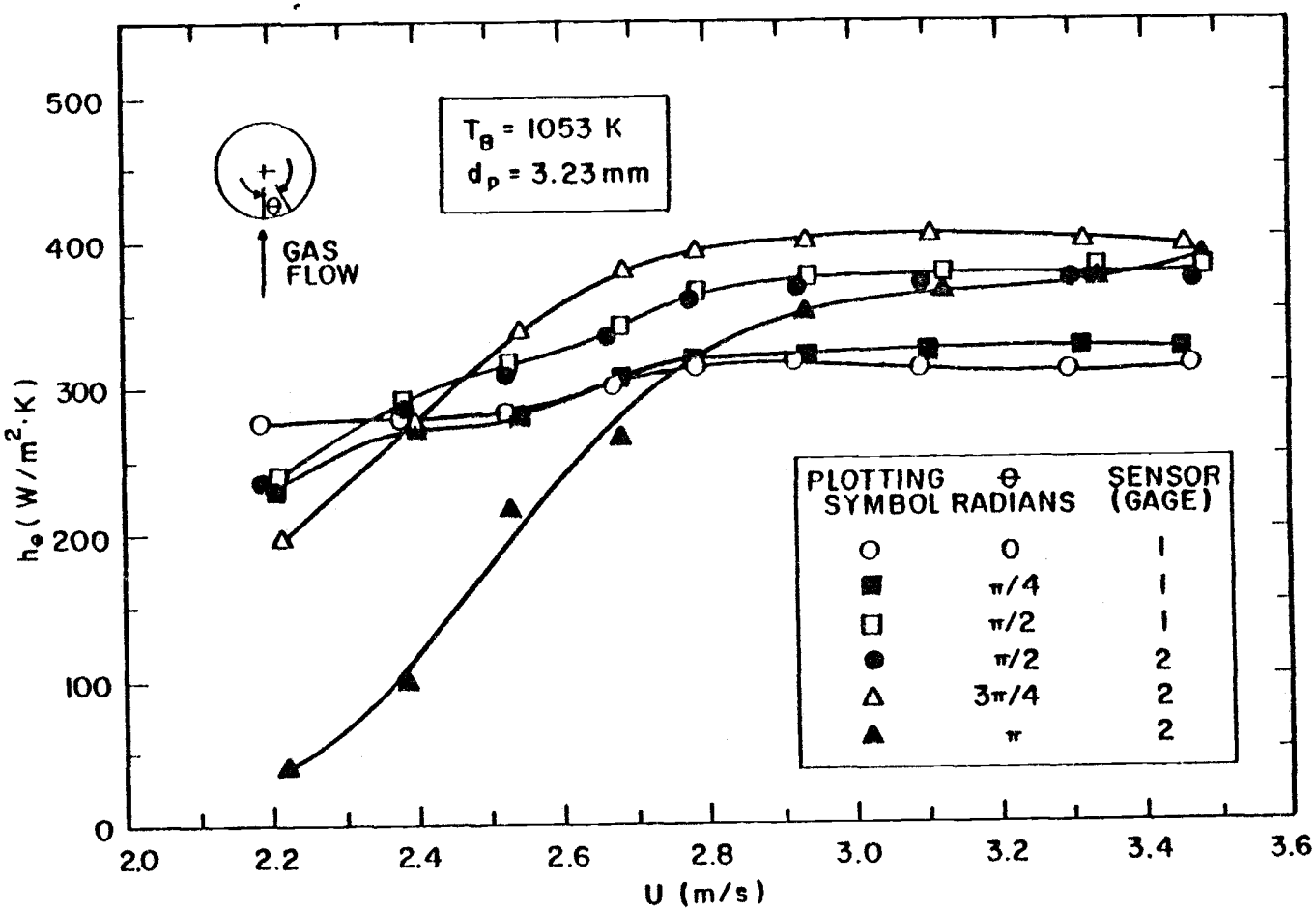

Figure 4.1 Local heat transfer coefficient vs. superficial velocity for d_p = 3.23 mm and T_B = 1053 K.

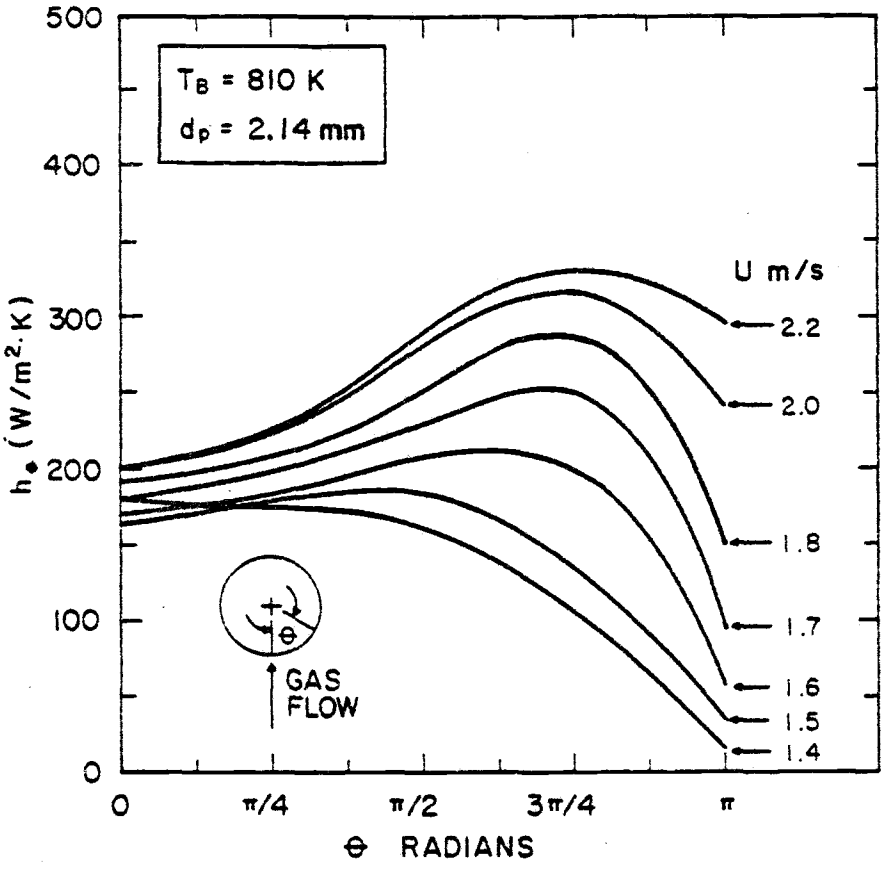

Figure 4.2 Local heat transfer coefficient vs. angular position for d_p = 2.14 mm and T_B = 810 K.

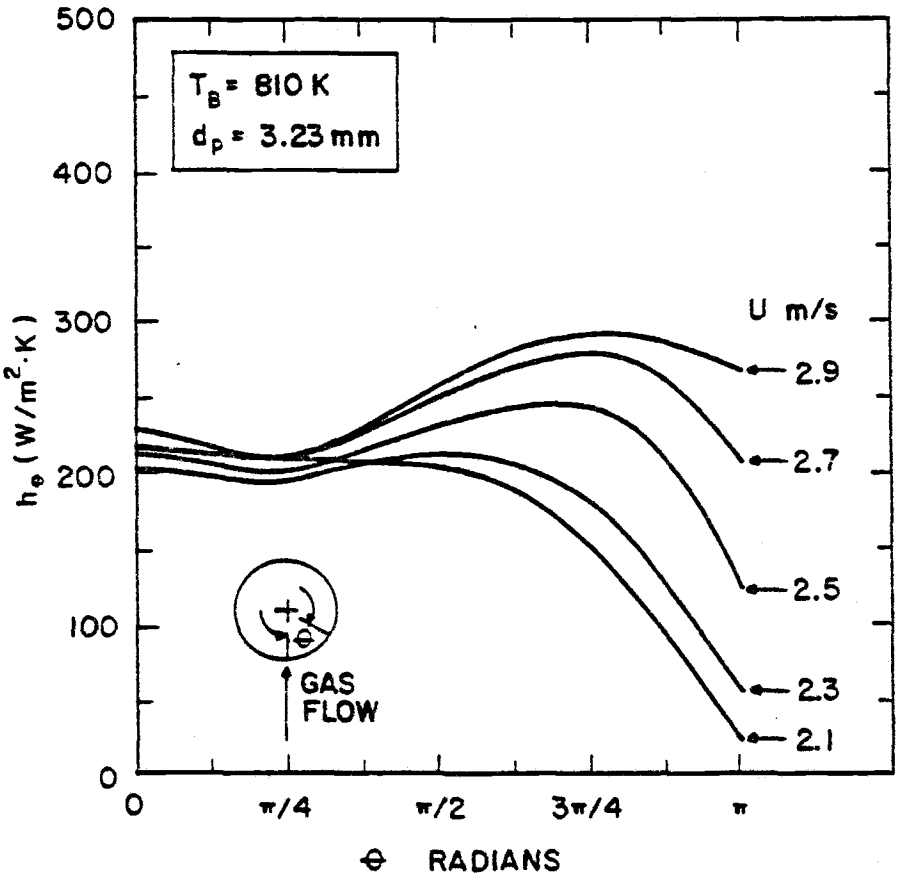

Figure 4.3 Local heat transfer coefficient vs. angular position for d_p = 3.23 and T_B = 810 K.

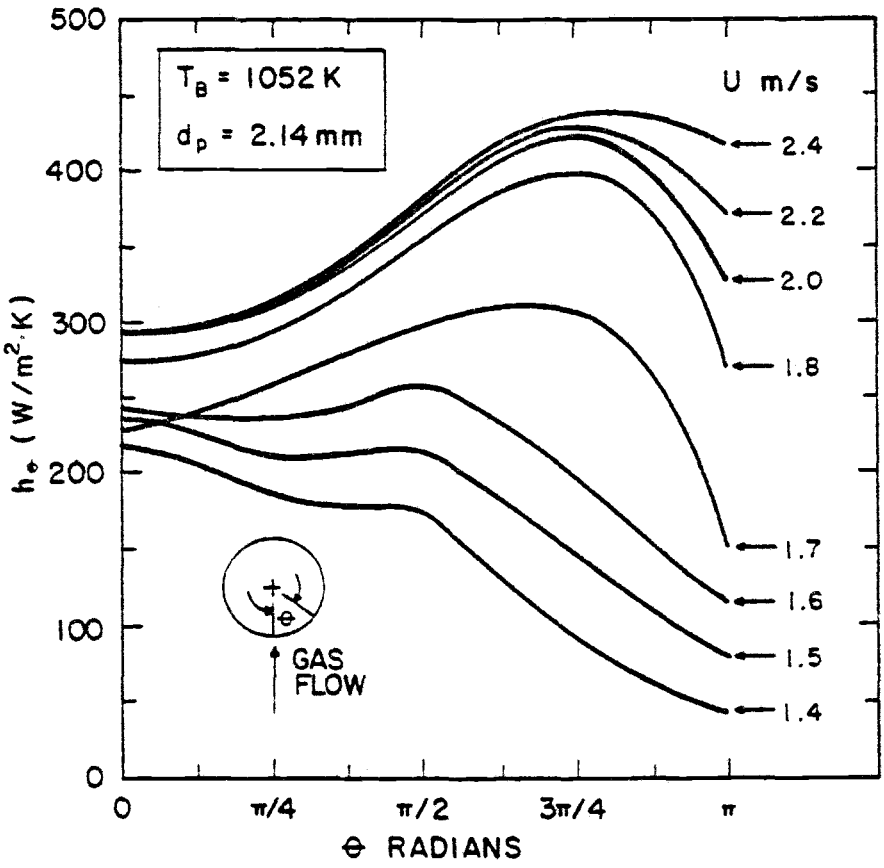

Figure 4.4 Local heat transfer coefficient vs. angular position for d_p = 2.14 mm and T_B = 1052 K.

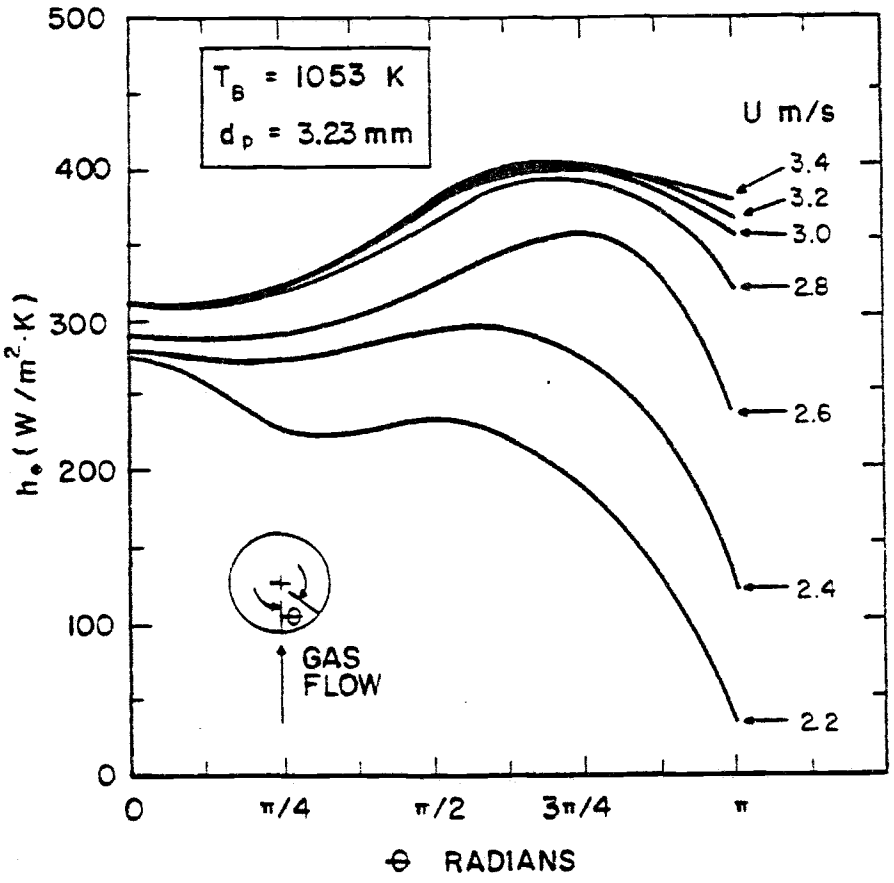

Figure 4.5 Local heat transfer coefficient vs. angular position for d_p = 3.23 mm and T_B = 1053 K.

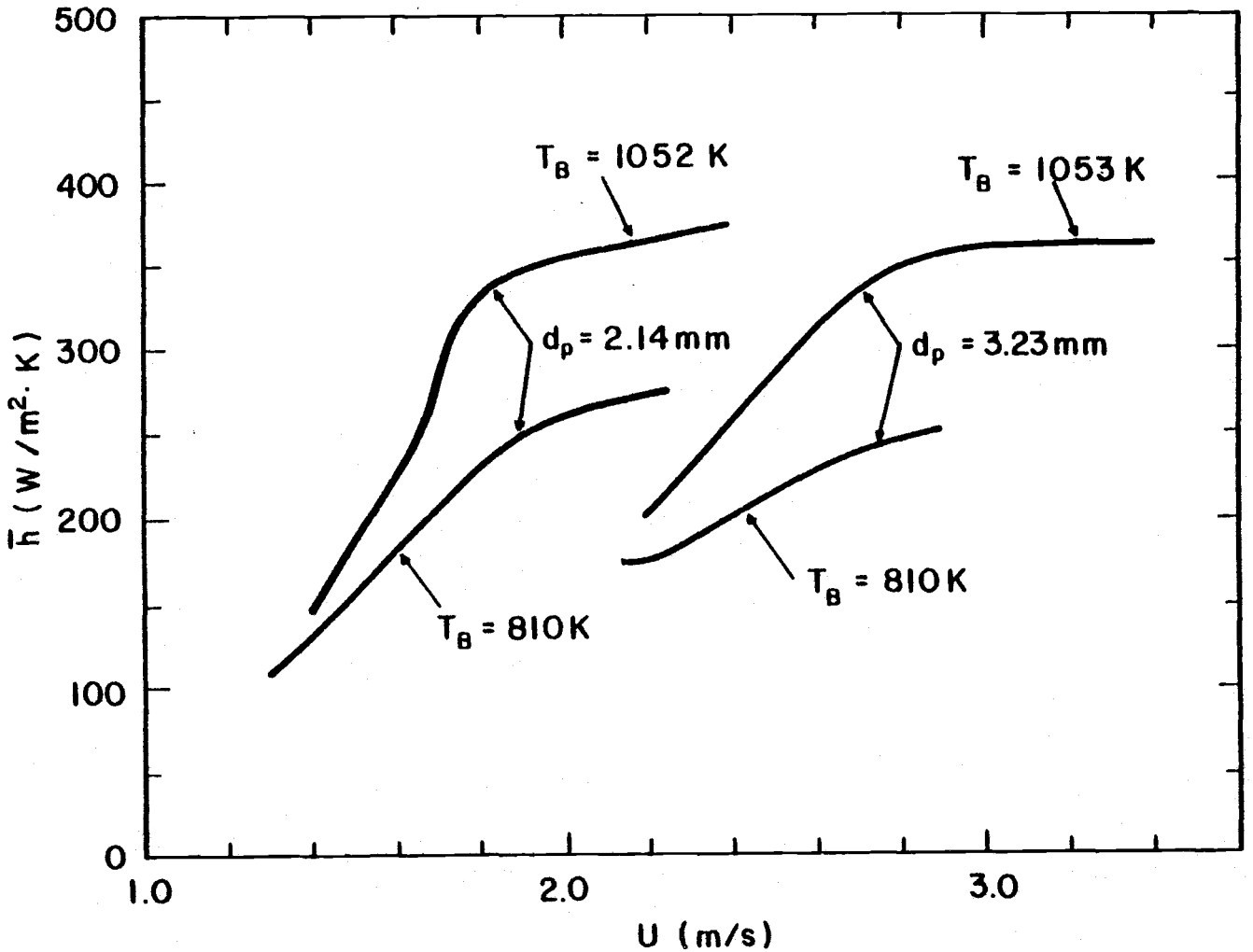

Figure 4.6 Spatial-average heat transfer coefficient vs. superficial velocity.

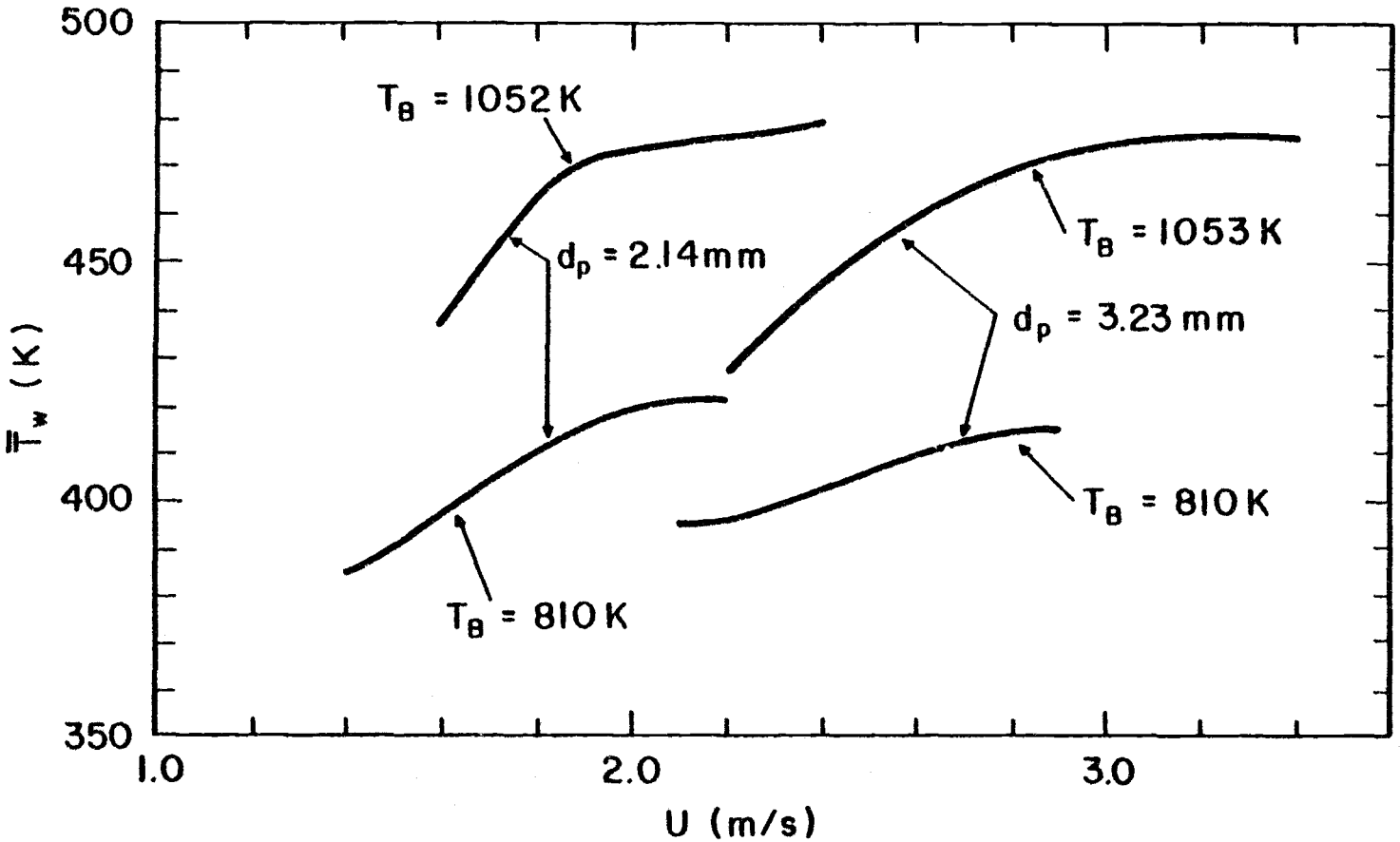

Figure 4.7 Spatial-average tube wall temperature at locations of heat transfer measurements vs. superficial velocity.

($\bar{T}_w$). This was computed by applying the trapezoidal rule to the local values of the surface temperature; which were obtained simultaneous with the local heat flux measurements.

4.2.2 Comments

Probably the most obvious trend present in the local heat transfer coefficient data is the very large (factor of ten or more) change in the magnitude of the coefficient, at the $\theta = \pi$ radian position, as the superficial gas velocity is varied. This is probably due to a relatively cool defluidized stack of particles, which remains on the top of the tube at low gas velocities. Intense bubbling, at higher gas velocities, displaces this defluidized stack of particles, and the local heat transfer coefficient increases greatly. This explanation is consistent with the hydrodynamic information (local voidage, emulsion residence time, visual inspection) available in the literature (Syromyatnikov et al., 1977; Glass and Harrison, 1964; Loew et al., 1979; Hager and Schrag, 1976; Gelperin and Einstein, 1971; Catipovic, 1979).

The local heat transfer coefficient at the $\theta = 0$ position is not a monotonic function of the superficial gas velocity. Rather, it tends to increase slightly as the gas velocity is reduced to, or below, minimum fluidization. This effect is known to occur in large particle fluidized beds ($d_p > 1$ mm) at near ambient temperature (Catipovic et al., 1978). The result had not been previously reported for high temperature conditions.

At least for the superficial velocity range considered, the distribution of the local heat transfer coefficient appears to approach an asymptotic limit as the velocity is increased. This is particularly noticeable with $d_p = 3.23$ mm and $T_B = 1053$ K (Figure 4.5); where the distribution of the local heat transfer coefficient is nearly identical for $U = 3.0$ m/s to $U = 3.4$ m/s. The trend is less noticeable for the other cases considered. The spatial average heat

transfer coefficient ($\bar{h}$) also approaches an asymptotic limit as the velocity is increased.

At both bed temperatures considered, the maximum value of $\bar{h}$ was higher for the smaller particles (d_p = 2.14 mm) than the larger particles (d_p = 3.23 mm). However, the differences are rather small: less than 4% at 1052 K and less than 10% at 810 K.

Difficulties related to the fluidized bed used in this study, which limit the accuracy of data taken near U_{mf}, or in packed beds, are: (1) large temperature gradients (several hundred degrees Kelvin) occur if the bed was packed or at U_{mf} for moderate periods of time (5 minutes); (2) distributor plate warpage caused uneven fluidization of the bed at or slightly below U_{mf}. At times, some bubbling appeared at one end of the bed, while the remainder of the bed was definitely packed.

The first difficulty was partially circumvented by taking data as soon as possible (45 seconds) after the desired superficial velocity was set. This allowed data to be taken while the bed temperature was still fairly well-defined. However, it is questionable if steady-state conditions were established under these operating conditions.

Heat transfer results obtained, in packed beds or near U_{mf}, are unreliable. Neither of the above-mentioned difficulties was significant at higher gas velocities when the bed was bubbling uniformly.

The spatial-average heat transfer coefficient ($\bar{h}$) attains a higher maximum value for the higher bed temperature considered. Radiant heat transfer between bed and tube is increased at high bed temperatures. The thermal conductivity of the gas also increases with increasing bed temperature.

4.2.3 Comparison of Present Results with Other Data

Little heat transfer information is available in the literature for the geometry, particle size range, and bed temperatures

considered here.

Fluidized bed combustor studies, employing horizontal tube arrays, and similar size particles to those used in the present study, generally give lower values for $\bar{h}_{MAX}$ than obtained here. A comparison of present data for $\bar{h}_{MAX}$ with fluidized bed combustor studies (Tang and Howe, 1980; Leon et al., 1979; Goblirsch et al., 1980; Wright et al., 1970) is given in Figure 4.8. All data shown were obtained using refractory particles (dolomite, limestone or "crushed refractory") and bed temperatures between 1046 K and 1173 K.

At low bed temperatures (approximately 310 K), tube arrays, at least for tubes internal to the array, give lower values for $\bar{h}_{MAX}$ than single horizontal tubes (Catipovic, 1979; Lese and Kermode, 1972). While no suitable data are available, it is plausible that the reduction of $\bar{h}_{MAX}$ for a tube array may be even larger at high bed temperature; where radiant heat transfer becomes significant (Botterill and Sealey, 1970; Baskakov et al., 1973b). Due to intense bubbling, a given tube in an array will "see" the relatively cool neighboring tubes, as well as the high temperature emulsion. This will give a lower radiant heat transfer, for a tube in an array, than for a single tube. The data of Leon et al. (1979), for a single horizontal tube, compare well with the present study.

Grewal and Saxena (1981) have written a comprehensive paper on the topic of maximum heat transfer coefficients for single horizontal tubes immersed in fluidized beds. They emphasized small particle beds (d_p < 1 mm), but present some data for large particle beds (obtained other literature) as well. For all data considered, they found good correlation between $\overline{Nu}_{MAX}$ and Ar. While Grewal and Saxena recommend their own more complex correlation, the earlier correlation due to Zabrodsky et al. (1974) and shown below fits the available data nearly as well.

$$\overline{Nu}_{MAX} = 0.88\ Ar^{0.213} \qquad (4.1)$$

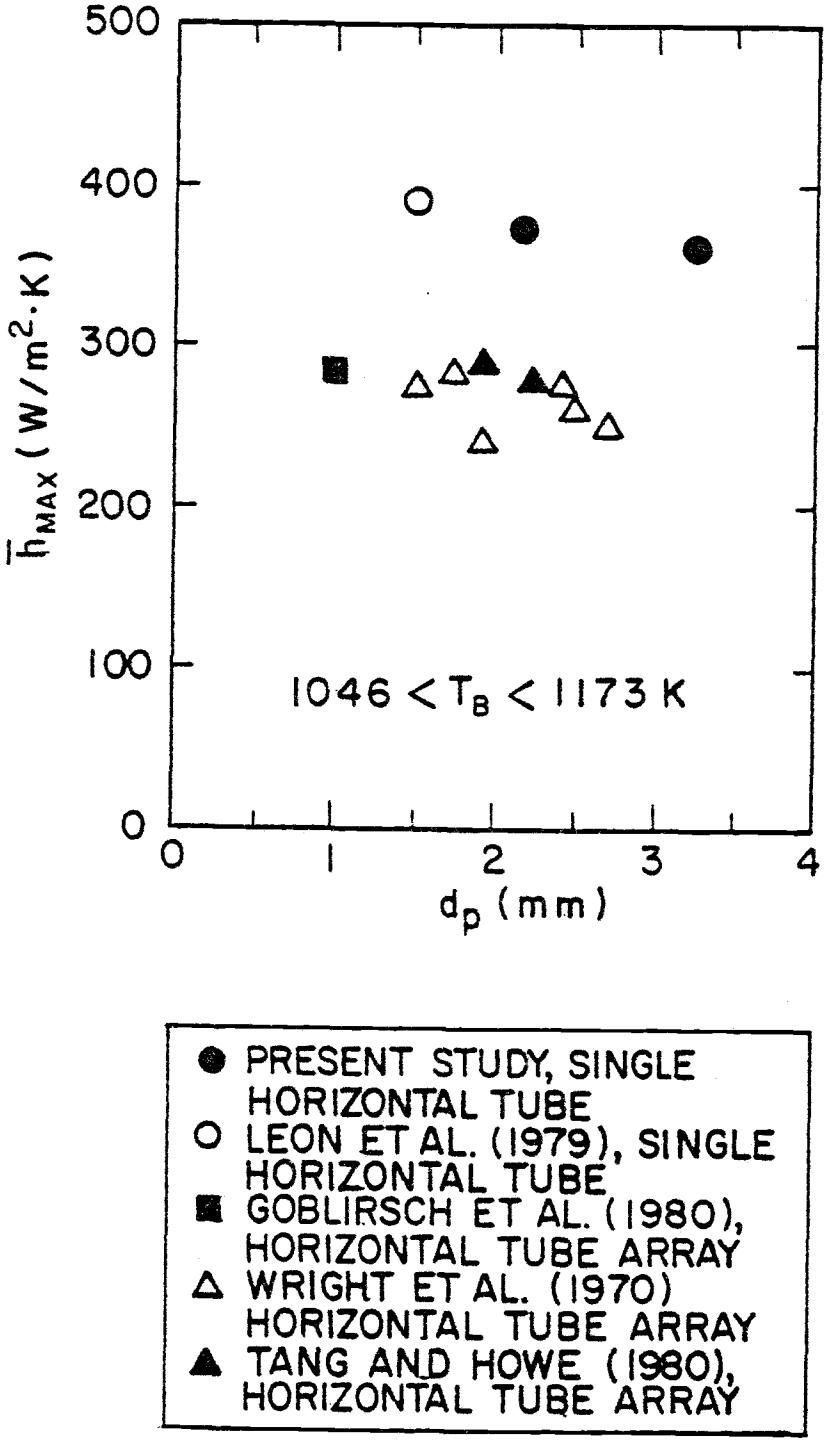

Figure 4.8 Maximum spatial-average heat transfer coefficient vs. average particle diameter for several studies.

Extrapolation of this correlation to values of Ar greater than 10^5 is risky, since that is the highest value of Ar considered by Grewal and Saxena.

For the high Archimedes number range, Baskakov et al. (1973a,b) recommend the following correlations:

$$\overline{Nu}_{MAX} = 0.86\ Ar^{0.20}\ ,\ 10^2 < Ar < 2x10^5 \qquad (4.2)$$

$$\overline{Nu}_{MAX} = 0.21\ Ar^{0.32}\ ,\ 2x10^5 < Ar < 10^8 \qquad (4.3)$$

Almost all of the data correlated by Zabrodsky et al. (1974) and Baskakov et al. (1973a,b) were obtained at near ambient temperature with air as a fluidizing gas. The above correlations, along with other high Archimedes number data, are compared with results of the present study in Figure 4.9. All gas (air) properties have been evaluated at the bed temperature. Property data were obtained from Touloukian et al. (1970; 1975).

The thermal conductivity and viscosity, for the products of complete combustion of propane, were computed using the equation given by Wilke (1950); which was suggested for such use by White (1974). Dissociation was neglected. Botterill and Teoman (1980) also neglected dissociation when performing similar calculations. For the complete range of excess air ratio and combustion chamber exit temperatures encountered in this study, properties of the combustion products were found to be within 4% of those of air at the same temperature. Properties of the constituent gases, in the combustion products, are presently known to only 5 or 10% accuracy (Touloukian et al., 1970; 1975). Therefore, with no real loss of precision, properties of air have been used in the data reduction. Westmoreland (1954) conducted an experimental study to measure the viscosity of several exhaust gases at elevated temperatures (up to 1373 K). He found the viscosity of the exhaust gases to be within a few percent of that of air at the same temperature.

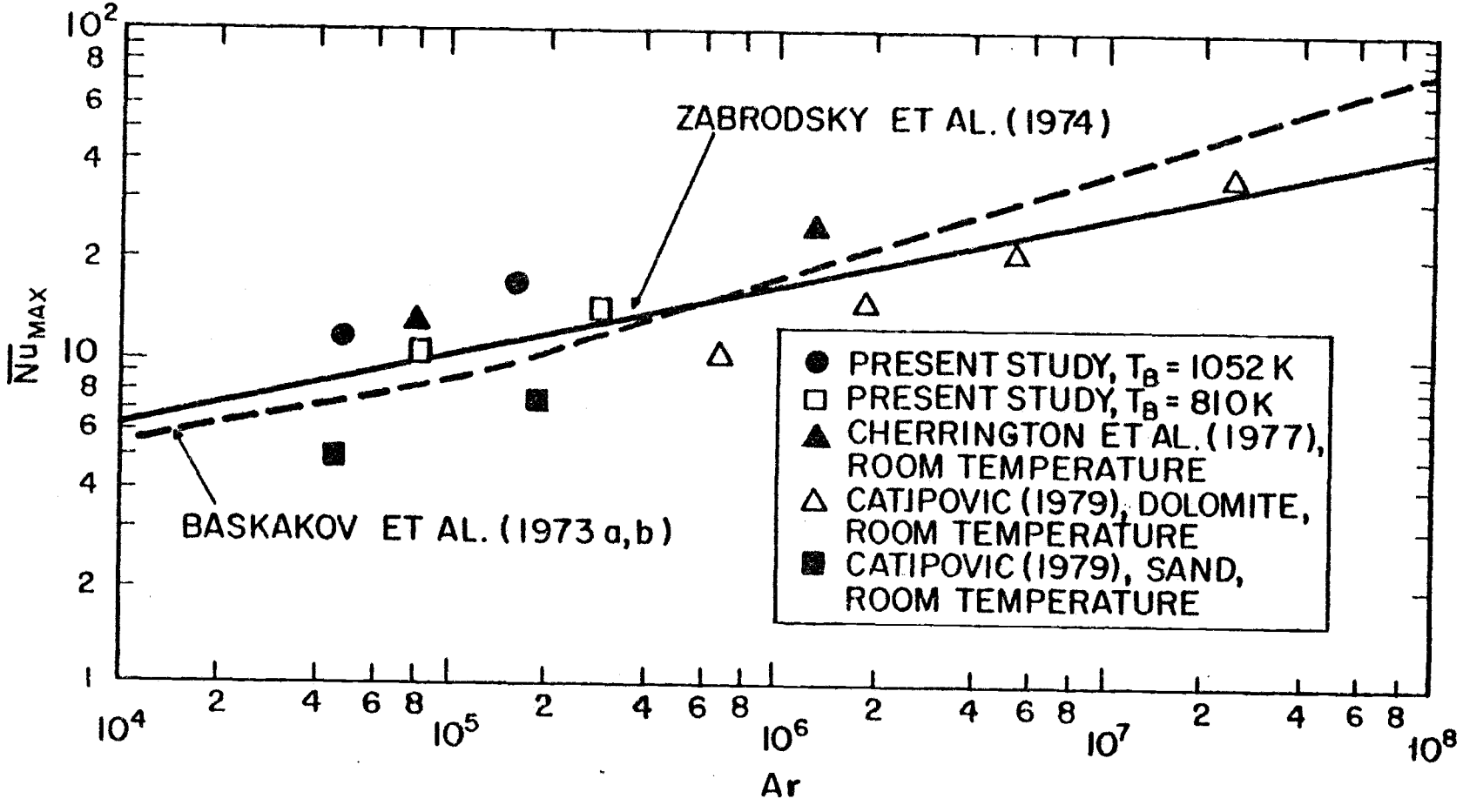

Figure 4.9 Maximum spatial-average Nusselt number vs. Archimedes number data for several studies.

The presence of radiant heat transfer tends to increase $\overline{Nu}_{MAX}$ over that attainable at the same value of Ar without radiant heat transfer. Data taken at high temperature tend to give higher values of $\overline{Nu}_{MAX}$.

Chandran et al. (1980) present heat transfer data for a horizontal tube in a large particle low temperature pressurized fluid-bed. However, they fail to specify a bed temperature or sufficient information from which the bed temperature could be estimated. Their data could not be used in the comparison shown in Figure 4.9.

In conclusion, available data are insufficient to either validate or invalidate the result of the present study.

V. CONCLUSIONS AND RECOMMENDATIONS FOR FUTURE WORK

5.1 Conclusions

An instrumented tube, for the measurement of time-average local heat transfer rate and time-average local surface temperature, was described in Chapter III. The commercially available Micro-Foil Heat Flow Sensor, with surface temperature thermocouple, was used. Heat transfer measurements with excellent repeatability were made with the device.

In Chapter IV experimental results for the time-average local heat transfer coefficient, to a single horizontal tube in a large particle (d_p = 2.14 mm and d_p = 3.23 mm) fluidized bed at elevated temperature (T_B = 810 K and T_B = 1053 K), were presented. The superficial gas velocity ranged from that required for minimum fluidization, or slightly packed, to the velocity where slugging first occurred, or the highest velocity air blower capacity would allow. The following conclusions are suggested:

a. As the superficial gas velocity is increased from that required for minimum fluidization, a large increase in the local heat transfer coefficient at the top of the tube ($\theta = \pi$) occurs. This is probably due to the presence of a defluidized stack of particles, on top of the tube, which is displaced by intense bubbling at higher gas velocities.

b. At least for the superficial velocity range considered, the distribution of the local heat transfer coefficient (i.e., h_θ vs. θ) appears to approach an asymptotic limit as the velocity is increased. Small changes in gas velocity, near the maximum velocity considered, yield small changes in the distribution of the local heat transfer coefficient.

c. The maximum spatial-average heat transfer coefficient ($\bar{h}_{MAX}$) was higher for the smaller particle (d_p = 2.14 mm) at both bed temperatures. However, the differences were rather small: 4% at T_B = 1052 K and 10% at T_B = 810 K.

d. For both particle sizes used, the maximum spatial-average heat transfer coefficient ($\bar{h}_{MAX}$) was higher at T_B = 1052 K than at T_B = 810 K. This is probably due to the increased thermal conductivity of the gas and increased radiant heat transfer at the higher bed temperature.

e. At minimum fluidization, or when the bed was slightly packed, nonuniform fluidization, i.e., uneven bubbling, and large temperature gradients in the bed, made heat transfer measurements taken under these conditions unreliable. Neither of these difficulties were present at higher gas velocities.

f. It was found that available heat transfer results, in the literature, were inadequate to either validate or invalidate the results of the present study.

5.2 Recommendations for Future Work

It would be highly desirable to perform a calibration check on the Micro-Foil Heat Flow Sensors, for a range of surface temperatures, after the sensors are mounted and the instrumented tube assembled. Limitations imposed by time, and available funding, prohibited such a calibration technique from being developed during the present study.

In the area of heat transfer to immersed tubes in large particle fluidized beds at elevated temperature, much experimental work remains to be performed.

There exists a need for detailed hydrodynamic information

(voidage, bubble fraction, emulsion residence time) for regions of the fluidized bed near the tube. This information is required to allow validation of some of the current analytical models of fluidized bed heat transfer; e.g., the Adams-Welty Model (Adams, 1977; Adams and Welty, 1979). Ideally, such measurements should be made in conjunction with simultaneous local heat transfer measurements.

Finally, hydrodynamic and heat transfer measurements should be made for tube arrays; if possible, under large-scale pilot plant conditions.

BIBLIOGRAPHY

Adams, R. L., "Analytical Model of Heat Transfer to a Horizontal Cylinder in a Gas Fluidized Bed," Ph.D. thesis, Oregon State University, Corvallis, Oregon (1977).

Adams, R. L., and J. R. Welty, "A Gas Convection Model of Heat Transfer in Large Particle Fluidized Beds," AIChE J., 25, 395 (1979).

Analog Devices, Inc., Norwood, Connecticut, ADIO Card Library, AIM03 Analog Input Card Manual (1980a).

_____, MacSym 2 System Manual (1980b).

ASME, "Flow Measurement," Power Test Codes, PTC 19.5, Ch. 4 (1959).

ASTM, "Standard Method for Measurement of Heat Flux Using a Copper-Constantan Circular Foil Heat-Flux Gage," Annual Book of Standards, part 41, E511-73, 731 (1978).

Babu, S. P., B. Shah, and A. Talwalkar, "Fluidization Correlations for Coal Gasification Materials--Minimum Fluidization Velocity and Fluidized Bed Expansion Ratio," AIChE Symposium Series No. 176, 74, 176 (1978).

Bachman, R. C., J. T. Chambers, and W. H. Giedt, "Investigation of Surface Heat-Flux Measurements with Calorimeters," ISA Trans., 4, 143 (1965).

Baskakov, A. P., O. K. Vitt, V. A. Kirakosyan, V. K. Maskayev, and N. F. Filippovsky, "Investigation of Heat Transfer Coefficient Pulsations and of the Mechanism of Heat Transfer from a Surface Immersed into a Fluidized Bed," in La Fluidisation et Ses Applications--Congres International (1-5 Oct. 1973), Vol. 1, Cepadues, Toulouse, France (1973a).

Baskakov, A. P., B. V. Berg, O. K. Vitt, N. F. Filippovsky, V. A. Kirakosyan, J. M. Goldobin, and V. K. Majkaev, "Heat Transfer to Objects Immersed in Fluidized Beds," Powder Technology, 8, 273 (1973b).

Basu, P., "Bed-to-Wall Heat Transfer in a Fluidized Bed Coal Combustor," AIChE Symposium Series No. 176, 74, 187 (1978).

Berg, B. V., and A. P. Baskakov, "Investigation of Local Heat Transfer between a Fixed Horizontal Cylinder and a Fluidized Bed," Intern. Chem. Eng., 14, 440 (1974).

Bernis, A., F. Vergnes, P. Le Goff, and J. P. Mihe, "Une Sonde à Film Chaud pour Mesure Locale et Instantée du Coefficient de Transfert de Chaleur dans un Lit Fluidisé Gaz-Solide," Powder Technology, 17, 229 (1977a).

Bernis, A., F. Vergnes, and P. Le Godd, "Influence du Passage d'une Bulle sur le Coefficient Instantané de Transfert de Chaleur a une Paroi Immergée dans un Lit Fluidisé," Powder Technology, 18, 267 (1977b).

Botterill, J. S. M., Fluid-Bed Heat Transfer, Academic Press, New York (1975).

Botterill, J. S. M., and C. J. Sealey, Brit. Chem. Eng., 15, 1167 (1970).

Botterill, J. S. M., and Y. Teoman, "Fluid-Bed Behavior at Elevated Temperatures," in Fluidization--Proceedings of the 1980 International Fluidization Conference, Henniker, New Hampshire, 3-8 Aug. 1980, edited by J. R. Grace and J. M. Matsen, Plenum Press, New York (1980).

Brown, E. A., R. J. Charlson, and D. L. Johnson, "Steady-State Heat Flux Gauge," Rev. Sci. Inst., 32, 984 (1961).

Catipovic, N. M., "Heat Transfer to Horizontal Tubes in Fluidized Beds: Experiment and Theory," Ph.D. thesis, Oregon State University, Corvallis, Oregon (1979).

Catipovic, N. M., T. J. Fitzgerald, and G. Jovanovic, "A Study of Heat Transfer to Immersed Tubes in Fluidized Beds," paper 28e, AIChE 71st Annual Meeting, Miami, Florida (12-16 Nov. 1978).

Chandran, R., J. C. Chen, and F. W. Staub, "Local Heat Transfer Coefficient around Horizontal Tubes in Fluidized Beds," J. Heat Transfer, 102, 152 (1980).

Cherrington, D. C., L. P. Golan, and F. G. Hammitt, "Industrial Application of Fluidized Bed Combustion--Single Tube Studies," in The Proceedings of the Fifth International Conference on Fluidized Bed Combustion (12-14 Dec. 1977), Vol. III, p. 184, MITRE Corp., McLean, Virginia (1978).

Chung, B. T. F., L. F. Fan, and C. L. Hwang, "A Model of Heat Transfer in Fluidized Beds," J. Heat Transfer, 94, 105 (1972).

Cranfield, R. R., and D. Geldart, "Large Particle Fluidization," Chem. Eng. Sci., 29, 935 (1974).

Doeblin, E. O., Measurement Systems Application and Design, Revised edition, McGraw-Hill, New York (1975).

Doichev, K., and N. S. Akhmakov, "Fluidisation of Polydisperse Systems," Chem. Eng. Sci., 34, 1357 (1979).

Fitzgerald, T. J., N. M. Catipovic, and G. N. Jovanovic, "Instrumented Cylinder for Studying Heat Transfer to Immersed Tubes in Fluidized Beds," Ind. Eng. Chem. Fundam., 20, 82 (1981).

Gardon, R., "An Instrument for the Direct Measurement of Intense Thermal Radiation," Rev. Sci. Inst., 24, 366 (1953).

_____, "A Transducer for the Measurement of Heat-Flow Rate," J. Heat Transfer, 82, 396 (1960).

Gelperin, N. I., and V. G. Einstein, "Heat Transfer in Fluidized Beds," in Fluidization, edited by J. F. Davidson and D. Harrison, Academic Press, New York (1971).

Glass, D. H., and D. Harrison, "Flow Patterns Near a Solid Obstacle in a Fluidized Bed," Chem. Engr. Sci., 19, 1001 (1964).

Goblirsch, G., R. H. Vander Molen, K. Wilson, and D. Hajicek, "Atmospheric Fluidized Bed Combustion Testing of North Dakota Lignite," Combustion Power Co., Inc., Menlo Park, California (May 1980).

Gosmeyer, C. D., "An Experimental Study of Heat Transfer in a Large Particle Heated Fluidized Bed," M.S. thesis, Oregon State University, Corvallis, Oregon (1979).

Grewal, N. S. and S. C. Saxena, "Maximum Heat Transfer Coefficient Between a Horizontal Tube and a Gas-Solid Fluidized Bed," Ind. Eng. Chem. Process Des. Dev., 20, 108 (1981).

Hager, N. E., "Thin Foil Heat Meter," Rev. Sci. Inst., 36, 1564 (1965).

Hager, W. R., and S. D. Schrag, "Particle Circulation Downstream from a Tube Immersed in a Fluidized Bed," Chem. Eng. Sci., 31, 657 (1976).

Hamming, R. W., Numerical Methods for Scientists and Engineers, McGraw-Hill, New York (1973).

Hornbaker, D. R., and D. L. Rall, "Thermal Perturbations Caused by Heat-Flux Transducers and Their Effect on the Accuracy of Heating-Rate Measurements," ISA Trans., 3, 123 (1964).

Kays, W. M., Convective Heat and Mass Transfer, McGraw-Hill, New York (1966).

Kline, S. J., and F. A. McClintock, "Describing Uncertainties in Single-Sample Experiments," Mech. Eng., 75, 3 (1953).

Kunii, D., and O. Levenspiel, Fluidization Engineering, John Wiley and Sons, New York (1969).

Leon, A. M., P. J. Choksey, and S. A. Bunk, "Design, Construction, Operation and Evaluation of a Prototype Culm Combustion Boiler/Heater Unit," report FE-3269-9A, Dorr-Oliver, Inc., Stamford, Connecticut (April 1979).

Lese, H. K., and R. I. Kermode, "Heat Transfer from a Horizontal Tube to a Fluidized Bed in the Presence of Unheated Tubes," Canadian J. Chem. Eng., 50, 44 (1972).

Loew, O., B. Schmutter, and W. Resnick, "Particle and Bubble Behavior and Velocities in a Large-Particle Fluidized Bed with Immersed Obstacles," Powder Technology, 22, 45 (1979).

Petrie, J. C., W. A. Freeby, and J. A. Buckham, "In-Bed Heat Exchangers," Chem. Eng. Prog., 64, 45 (1968).

Pikashov, V. S., A. I. Ilchenko, G. P. Kuchin, and I. F. Zemskiy, "A Method for Checking the Hypothesis of Additivity of Components of Combined Conductive, Convective and Radiative Heat Transfer in Two-Phase Flow," Heat Transfer--Soviet Research, 12, 124 (1980).

Samson, T., "Heat Transfer to Objects in Fluidized Beds," in La Fluidisation et Ses Applications--Congres International (1-5 Oct. 1973), Vol. 1, Capadues, Toulouse, France (1973).

Saxena, S. C., N. S. Grewal, J. D. Gabor, S. S. Zabrodsky, and D. M. Galershtein, "Heat Transfer between a Gas Fluidized Bed and Immersed Tubes," in Advances in Heat Transfer, Vol. 14, edited by T. F. Irvine and J. P. Hartnett, Academic Press, New York (1978).

Schulte, E. H., and R. F. Kohl, "A Transducer for Measuring High Heat Transfer Rates," Rev. Sci. Inst., 41, 1732 (1970).

Skinner, D. G., The Fluidised Combustion of Coal, Mills and Boon Ltd., London (1971).

Syromyatnikov, N. I., V. M. Kulikov, and V. N. Korolev, "Structural and Hydrodynamic Conditions of Fuel Combustion in a Low-Temperature Fluidized Bed," J. Inst. Fuel, 50, 169 (1977).

Tang, J. T., and W. Howe, "Heat Transfer Analyses for the 6'x6' Atmospheric Fluidized Bed Development Facility," paper 80-HT-128, Joint ASME/AIChE National Heat Transfer Conference, Orlando, Florida, 27-30 July (1980).

The Babcock and Wilcox Co., "Fluidized Bed Combustion Development Facility and Commercial Utility AFBC Design Assessment," B and W Contract CRD-3054, Alliance, Ohio, monthly progress report for August (1979).

Thrasher, L. W., and R. C. Binder, "A Practical Application of Uncertainty Calculations to Measured Data," Trans. ASME, 79, 373 (1957).

Touloukian, Y. S., P. E. Liley, and S. C. Saxena, Thermophysical Properties of Matter, Vol. 3, IFI/Plenum, New York (1970).

Touloukian, Y. S., S. C. Saxena, and P. Hestermans, Thermophysical Properties of Matter, Vol. 11, IFI/Plenum, New York (1975).

Welty, J. R., "Heat Transfer in High Temperature Fluidized Beds with Immersed Tubes for Coal Combustion Service," Annual Report Oct. 1977 to Sept. 1978, U.S. Dept. of Energy report FE-2714-5, (1978).

Westkaemper, J. C., "On the Error in Plug-Type Calorimeters Caused by Surface-Temperature Mismatch," J. Aero. Sci., 28, 907 (1961).

Westmoreland, J. C., "Determination of Viscosity of Exhaust-Gas Mixtures at Elevated Temperatures," NACA TN 3180 (1954).

White, F. M., Viscous Fluid Flow, McGraw-Hill, New York (1974).

Wilke, C. R., "A Viscosity Equation for Gas Mixtures," J. Chem. Phys., 18, 517 (1950).

Woodruff, L. W., L. F. Hearne, and T. J. Keliher, "Interpretation of Asymptotic Calorimeter Measurements," AIAA J., 5, 795 (1967).

Wright, S. J., H. C. Ketley, and R. G. Hickman, "The Combustion of Coal in Fluidized Beds for Firing Shell Boilers," J. Inst. Fuel, 42, 235 (1969).

Wright, S. J., R. Hickman, and H. C. Ketley, "Heat Transfer in Fluidised Beds of Wide-Size Spectrum at Elevated Temperatures," Brit. Chem. Eng., 15, 1551 (1970).

Zabrodsky, S. S., Hydrodynamics and Heat Transfer in Fluidized Beds, MIT Press, Cambridge, Massachusetts (1966).

Zabrodsky, S. S., N. V. Antonishin, G. M. Vasiliev, and A. L. Paranas, Vesti Akad. Nauk BSSR, ser Fiz-Energ. Nauk, No. 4, 103 (1974). (As cited by Grewal and Saxena, 1981.)

Zabrodsky, S. S., Yu. G. Epanov and D. M. Galershtein, "On the Dependence of Fluidized Bed-Wall Heat Transfer Coefficients on the Thermal Conductivity and Volumetric Heat Capacity of the Particles," in Fluidization--Proceedings of the Second Engineering Foundation Conference, Trinity College, Cambridge, England, 2-6 April 1978, edited by J. F. Davidson and D. L. Keairns, Cambridge University Press, Cambridge (1978).

Ziegler, E. N., L. B. Koppel, and W. T. Brazelton, "Effects of Solid Thermal Properties on Heat Transfer to Gas Fluidized Beds," Ind. Eng. Chem. Fundam., 3, 324 (1964).

APPENDICES

APPENDIX A

Error Analysis

The heat flux transducer, employed in this study, consists of a Micro-Foil Heat Flow Sensor (hereafter referred to as sensor) covered by a 0.127 mm thick stainless steel shim stock. Three sources of error are identified and their magnitudes estimated:

1. Heat conduction in the shim stock along the surface.
2. Disturbance of the thermal boundary layer due to nonuniform surface temperature.
3. The combination of 1 and 2 above along with calibration and data acquisition errors.

In operation, the heat flux signal was found to vary only about ±6% from its time-average value. Therefore, only a steady-state error analysis will be made. Time-average values will be used for all parameters.

A.1 Heat Conduction Along Surface

An analysis is performed to estimate the fraction of energy (heat flux), absorbed at the shim stock's upper surface, which is actually conducted to the sensor.

Since the shim stock is thin (0.127 mm), and made of relatively high thermal conductivity material, the temperature difference across its thickness will be neglected. The sensor is considered to represent a contact resistance (R_{GAGE}) between the shim stock and tube wall. A uniform convective boundary condition is assumed for the upper surface. The boundary condition around the periphery of the sensor is taken to be uniform temperature at T_{w2}. Boundary conditions

and coordinate system are given in Figure A.1.

The formulation of the problem is

$$\frac{\partial^2 T_w}{\partial x^2} + \frac{\partial^2 T_w}{\partial y^2} - \frac{(h_1+h_2)}{k_1\delta_1} T_w = -\frac{(h_1 T_B + h_2 T_{w2})}{k_1\delta_1}$$

Boundary conditions are

$$T_w(x_o,y) = T_{w2}$$

$$T_w(x,y_o) = T_{w2}$$

$$\frac{\partial T_w(x,0)}{\partial y} = 0$$

$$\frac{\partial T_w(0,y)}{\partial x} = 0$$

One quantity of interest is the ratio of heat flux transmitted to the sensor to that absorbed at the upper surface of the shim stock.

$$\frac{q_2}{q_1} = -\left(\frac{h_2}{h_1}\right)\left(\frac{T_w - T_{w2}}{T_w - T_B}\right)$$

Details of the solution, by the classical technique of separation of variables, are left to the reader.

Parameters used are as follows:

$$\delta_1 = 0.127 \text{ mm}$$

$$k_1 = 20.0 \text{ W/m}\cdot\text{K}$$

$$h_1 = 365 \text{ W/m}^2\cdot\text{K}$$

$$h_2 = \frac{1}{R_{GAGE}} = 1893 \text{ W/m}^2\cdot\text{K}$$

$$T_B = 1053 \text{ K}$$

$$T_{w2} = 363 \text{ K}$$

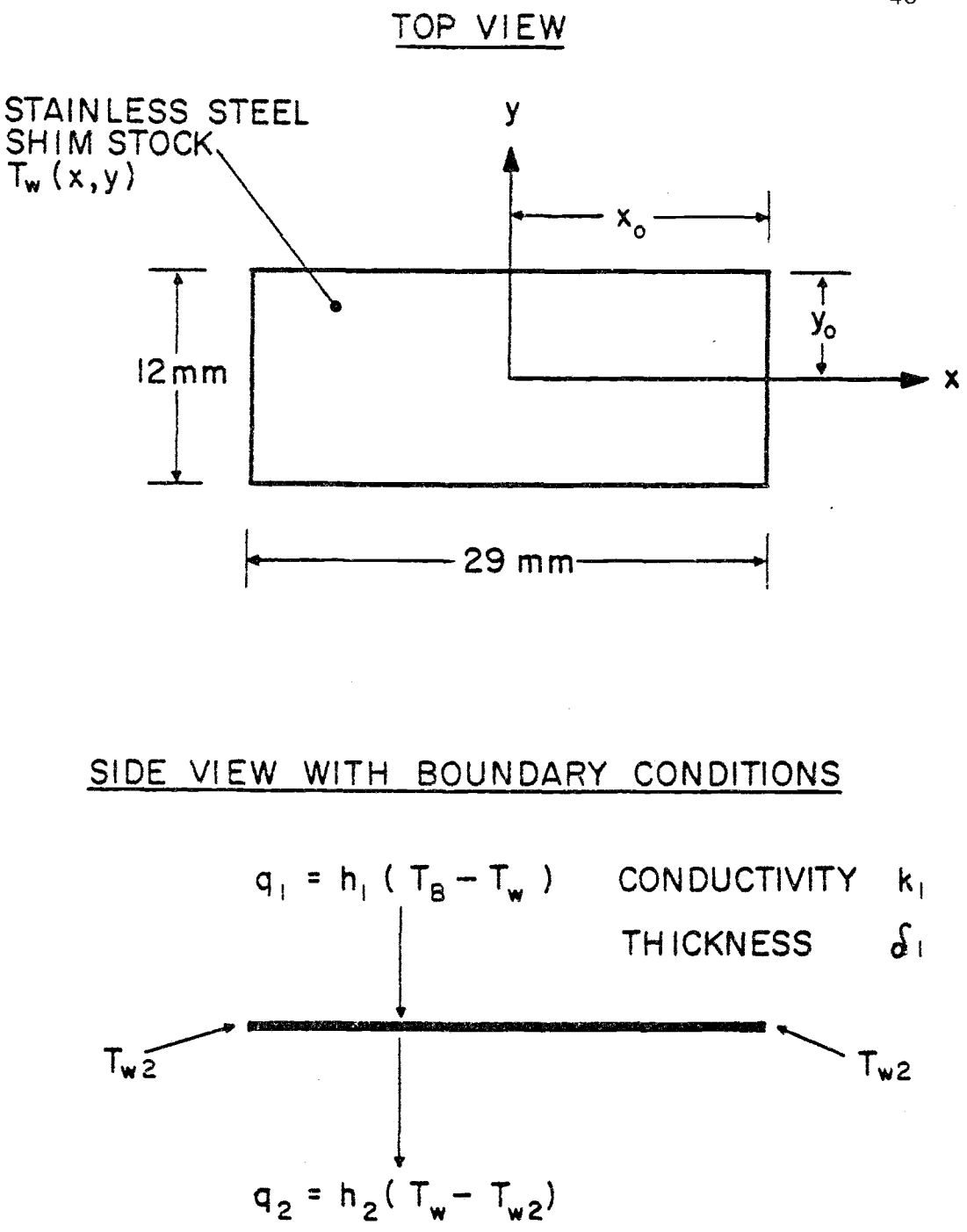

Figure A.1 Boundary conditions and coordinate system for heat conduction analysis.

The values of h_1, T_B and T_{w2} correspond to the $\theta = \pi/2$ radian position on the tube during a typical high temperature experiment. Values of q_2/q_1, over the active area of the sensor (where the thermocouple junctions are located) are shown in Figure A.2. About 98% of the heat flux absorbed at the shim stock's upper surface is conducted to the sensor's active area.

The surface temperature distribution , at $x = 0$, is shown in Figure A.3. This surface temperature is required for the thermal boundary layer analysis which follows.

A.2 Thermal Boundary Layer Analysis

For purposes of thermal boundary layer analysis, the surface temperature distribution is idealized somewhat as shown in Figure A.4. The point at which the boundary layer starts is a distance L ahead of the sensor's position. A laminar boundary layer was assumed.

The superposition technique, based on an integral solution for a step in surface temperature, described by Kays (1966), was used. Leaving details to the reader, only relevant results are presented here. The solution applies only when the surface is covered by gas bubbles, i.e., heat transfer by pure gas convection.

Of interest is the ratio of gas convective heat transfer coefficient for the nonuniform surface temperature (h_g), to the gas convective heat transfer coefficient for an isothermal surface (h_{Tg}). The ratio h_g/h_{Tg}, for the active area of the sensor, is shown in Figure A.5. Values of L used are near maximum for the experimental conditions encountered.

Flat plate flow gives lower values of h_g/h_{Tg} than stagnation point flow. As a worst probable case, the $L/y_o = 6$ flat plate case is taken and spatially averaged over the sensor active area.

$$\left(\frac{h_g}{h_{Tg}}\right)_{MAX} \doteq 0.75$$

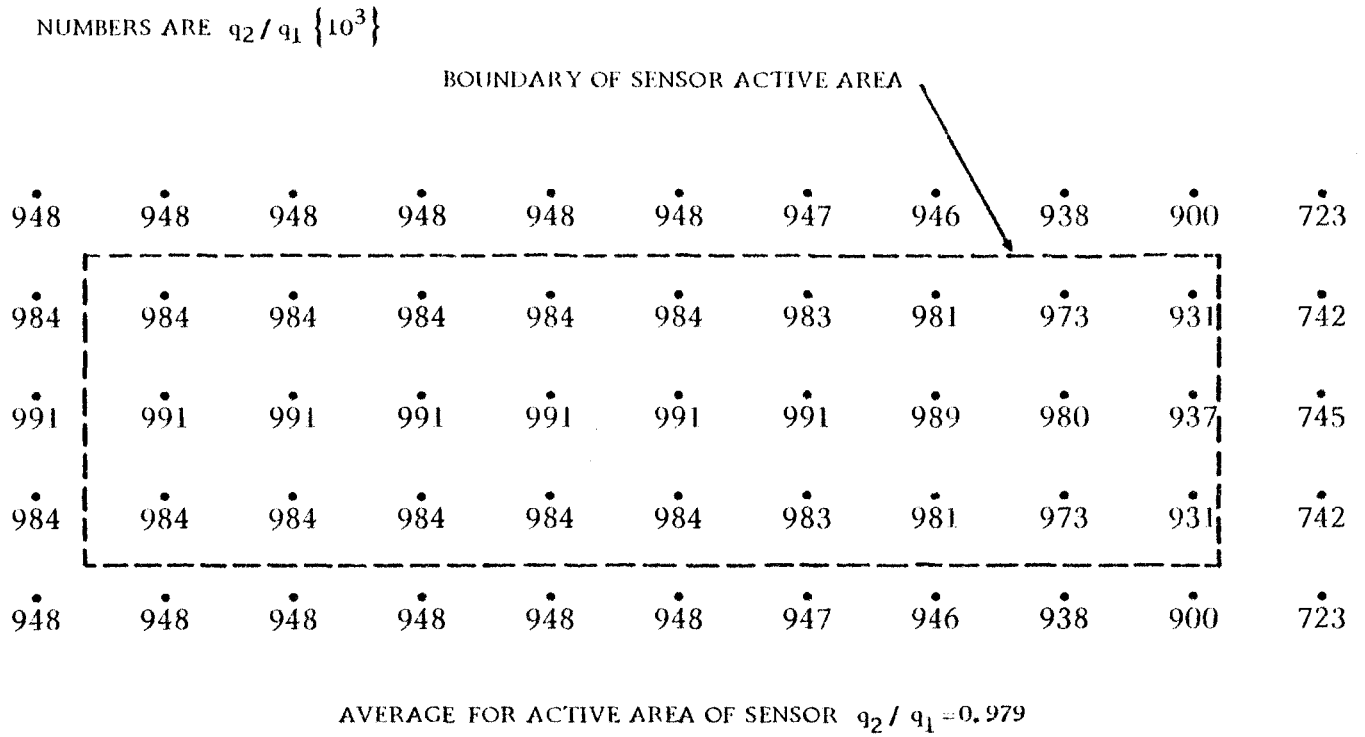

Figure A.2 Values of q_2/q_1 for the active area of the sensor.

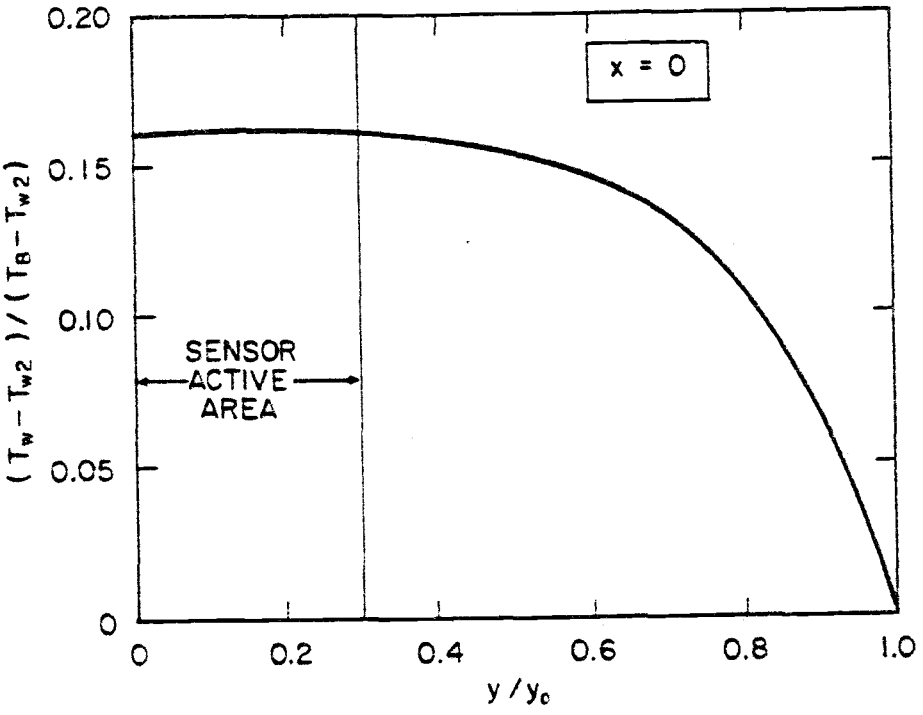

Figure A.3 Surface temperature distribution along the line x = 0.

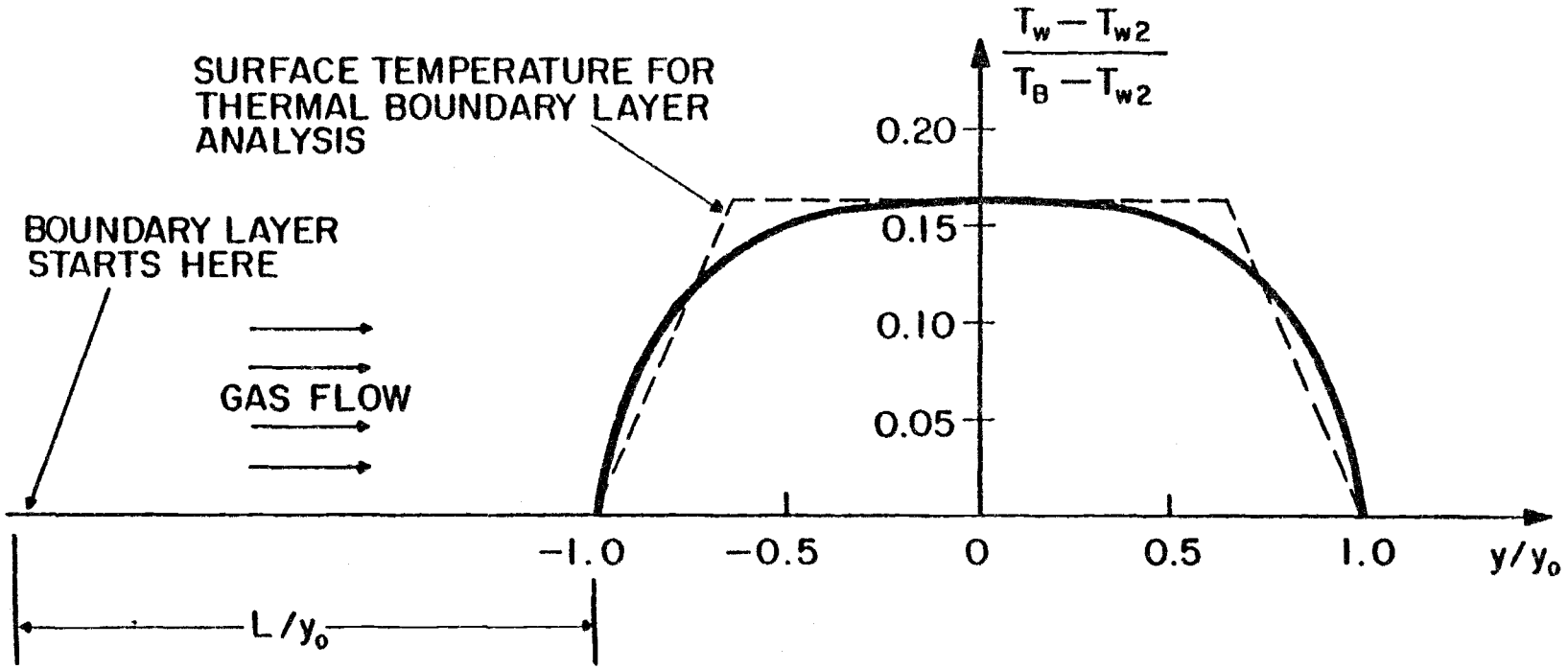

Figure A.4 Surface temperature distribution for thermal boundary layer analysis.

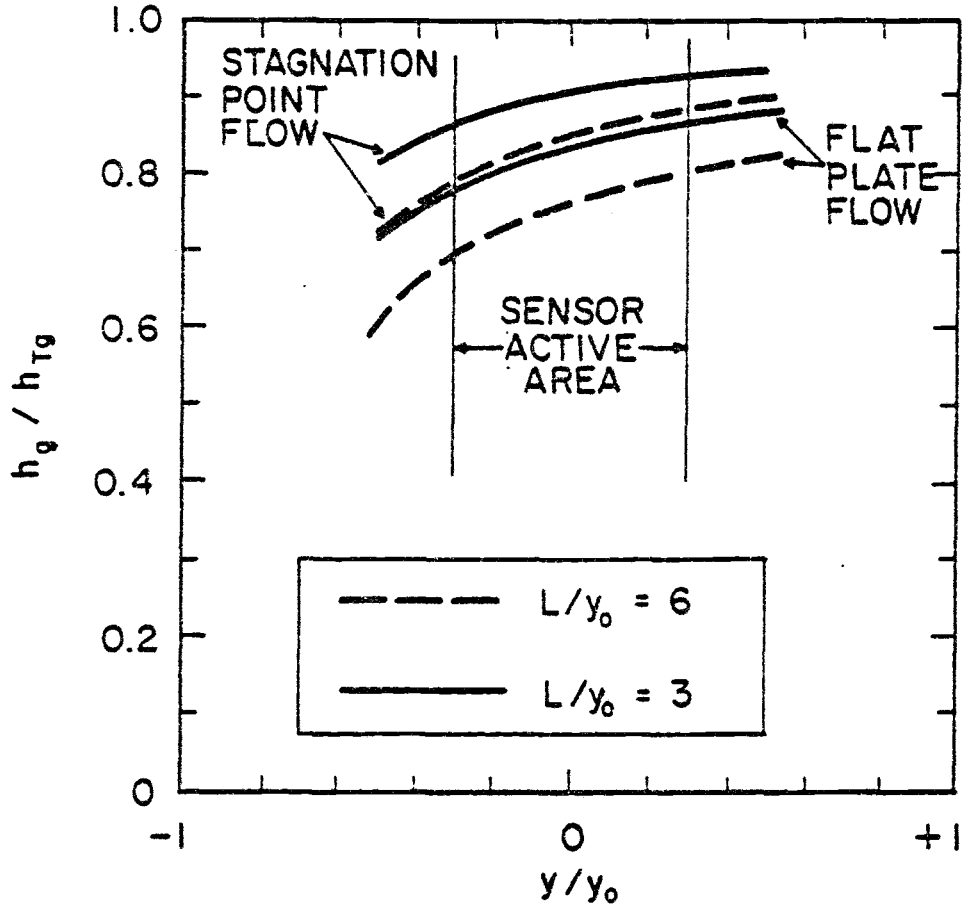

Figure A.5 Ratio of gas convective heat transfer coefficient for the nonuniform surface temperature to that for uniform surface temperature for the active area of the sensor.

In terms of relative error,

$$\left(\frac{h_g - h_{Tg}}{h_{Tg}}\right)_{MAX} \doteq -0.25$$

An estimate of the relative error in the spatial average heat transfer coefficient, due to thermal boundary layer disturbance, is obtained by multiplying the above relative error by the fraction of total heat transfer due to bubbles contacting the tube. This value is estimated from data given by Catipovic (1979) as 0.15. Therefore,

$$\left(\frac{\bar{h} - \bar{h}_T}{\bar{h}_T}\right)_{MAX} \doteq (0.15)(-0.25)$$

$$\doteq -0.04$$

The relative error in $\bar{h}$ could be as large as 4%. However, it is probably less. By mounting sensors side-by-side around half of the tube periphery, the nonuniformity in surface temperature, and the associated measurement error, would be largely eliminated.

It should be mentioned that all of Catipovic's heat transfer data were taken in a narrow (0.127 m wide) low temperature fluidized bed. Cranfield and Geldart (1974) note significant hydrodynamic differences between narrow two-dimensional beds and wider three-dimensional beds of large particles (d_p > 1 mm). The use of Catipovic's data for the fraction of total heat transfer due to bubbles is a rather crude approximation.

A relative error of 4%, for nonuniformity in surface temperature, will be used for the local heat transfer coefficient (h_θ) as well as for $\bar{h}$.

A.3 Estimated Error in the Local Heat Transfer Coefficient

The local heat transfer coefficient is given by

$$h_\theta = \frac{q_\theta}{T_B - T_{w\theta}} = \frac{CV_\theta}{T_B - T_{w\theta}}$$

where

C = calibration constant for the sensor at the given surface temperature

V_θ = voltage output of the sensor

For random calibration and data acquisition errors, the root-sum-square (RSS) error is given by Doeblin (1975); Thrasher and Binder (1957); and Kline and McClintock (1953).

$$\left(\frac{\Delta h_\theta}{h_\theta}\right)_{RAN} = \pm \left[\left(\frac{\Delta C}{C}\right)^2 + \left(\frac{\Delta V_\theta}{V_\theta}\right)^2 + \frac{(\Delta T_B)^2 + (\Delta T_{w\theta})^2}{(T_B - T_{w\theta})^2}\right]^{1/2}$$

Using manufacturers' specifications and operating experience, best estimates of the uncertainty for each quantity, for a typical high temperature experiment, are shown below.

$$\left(\frac{\Delta h_\theta}{h_\theta}\right)_{RAN} = \pm \left[(0.05)^2 + (0.05)^2 + \frac{(8.5)^2 + (3.5)^2}{(1053 - 478)^2}\right]^{1/2}$$

$$= \pm \left[(0.05)^2 + (0.05)^2 + (0.016)^2\right]^{1/2}$$

$$\doteq \pm \ 0.08$$

Errors in bed temperature and tube wall temperature contribute very little to the random error.

The inherent errors in the experiment, due to nonuniform surface temperature and heat conduction along the surface through the shim stock, analyzed in section A.1 and A.2, are now added to the random errors.

$$\left(\frac{\Delta h_\theta}{h_\theta}\right) = (+0.08, -0.08) + (0,-0.04) + (0,-0.02)$$

$$= (+0.08, -0.14)$$

It is improbable that the values of the local heat transfer coefficient reported are more than 8% higher or 14% lower than the actual values.

APPENDIX B

Data Reduction

Equations used in computing time-average values of the local heat flux, local surface temperature, and local heat transfer coefficient are given below. It is assumed the reader is familiar with simple analog data acquisition techniques.

For any data channel (includes instrumentation amplifier, FM data recorder, and analog-to-digital converter incorporated in the MacSym 2 data acquisition system), denoted by a subscript i, the relationship between transducer output voltage (either surface temperature thermocouple or thermopile type heat flux transducer), overall offset voltage, overall channel gain, and voltage output as given on the MacSym 2 system, is

$$V_{ti}^{j} = \frac{V_{OUTi}^{j} - V_{OSi}}{K_i} \qquad \text{in volts}$$

For example, let channel 3 correspond to the local surface temperature, and channel 4 correspond to the local heat flux, for a given condition. The surface temperature, at a time denoted by superscript j, is given by

$$T_{w3}^{j} = a_1 + a_2 e + a_3 e^2 + a_4 e^3 + a_5 e^4 \qquad \text{in } ^{\circ}C$$

where $e = V_{t3}^{j} (10^6)$ in μV

$a_1 = 0$

$a_2 = (2.56613)\ 10^{-2}$

$a_3 = (-6.19549)\ 10^{-7}$

$a_4 = (2.21816)\ 10^{-11}$

$a_5 = (-3.55009)\ 10^{-16}$

The above constants are given by Analog Devices (1980b) for copper-constantan thermocouples (type T) with an ice bath reference junction.

Local heat flux is given by

$$q_4^j = \frac{V_{t4}^j \, (3.154) \, 10^6}{S C_w^j} \qquad \text{in } W/m^2$$

where S = Micro-Foil Heat Flow Sensor calibration factor at 21°C, in $\mu V/(Btu/hr \cdot ft^2)$

C_w^j = dimensionless correction factor for surface temperature, a function of T_{w3}^j, given by

$$C_w^j = 0.85 - (0.09)D^j + (0.015)(D^j - 1)D^j$$

where $D^j = (T_{w3}^j - 93.667)/55.556$

The above equation for C_w^j and D^j is valid between 93°C and 215°C: the range of surface temperature encountered in this study.

Time-average values of local surface temperature and local heat flux are obtained by sampling, at a rate of about 12 samples per second per channel, and summing the instantaneous readings, then dividing by the total number of samples taken (N).

$$T_{w3} = \frac{1}{N} \sum_{j=1}^{N} T_{w3}^j$$

$$q_4 = \frac{1}{N} \sum_{j=1}^{N} q_4^j$$

Local heat transfer coefficient, for the condition considered, is given by

$$h_\theta = \frac{q_4}{T_B - T_{w3}} \qquad \text{in } W/m^2 \cdot K$$

Sixty seconds of data were sampled for each condition, i.e., about 720 samples per channel. Use of a larger number of samples did not improve the repeatability of the results.

For those at Oregon State University, the data reduction program used may be inspected, by listing the program DATARE.2 on the MacSym 2 system's CRT screen. Some documentation is provided, on the program listing, in the form of remark statements. The program mentioned is stored on the duplicate master diskette. It is strongly recommended that those conducting similar research write their own data reduction program(s), rather than use the existing one.

APPENDIX C

Test Procedure

The information presented in this appendix is of use only to those who will conduct future research at the same fluidized bed facility as used in this study.

It is assumed the reader has read the information in Welty (1978), has inspected, and is familiar with, the Oregon State University High Temperature Fluidized Bed Facility. Further, it is assumed the reader is familiar with simple analog data acquisition techniques.

Major steps, taken in the set-up and execution of an experiment, are given below. Potential hazards exist. The writer assumes no liability for the execution of the instructions given below, or for any omissions of relevant information.

1. Mount instrumented tube in desired mounting port on the test section.
2. Attach coolant lines to the instrumented tube.
3. Fill bed with particles.
4. Very important: Check that all the various pipe plugs and caps on the test section are tight. The 2½" pipe caps, on the test section, have, on occasion, been found loose (probably due to repeated expansion and contraction during operation). It could cause considerable discomfort for the operator if one of these caps came off when operating the fluidized bed at high temperatures!
5. Establish coolant flow through tube.
6. Light propane burner and warm-up fluidized bed according to instructions given by Welty (1978).

7. While bed is warming up, attach (solder) lead wires from the Micro-Foil Sensors to instrumentation amplifier input leads. Set-up reference junction and ice bath for the surface temperature thermocouples. Attach FM data recorder inputs to amplifier outputs. Make note of what type of data each channel corresponds to, e.g., channel 1 = heat flux on sensor 2.

8. After the bed is at the desired temperature, fluidize the bed to the maximum superficial velocity to be used. Set amplifier gains to give about 80% of full-scale deflection on each channel of the FM data recorder. Set amplifier offset to give a small positive offset voltage (about 0.05 volts at amplifier output).

9. For each velocity and angular position of interest, record heat flux and surface temperature data on the FM data recorder. Record bed temperature, venturi pressures, and flowing air temperature on the data sheet. Take the barometric pressure at some time during the run (needed in superficial velocity calculation). Adjust coolant and water flow rates as needed.

10. When all data at the given bed temperature have been taken, short all input leads with alligator clips. This will put the offset voltage, for each channel, on the FM tape.

11. Disconnect (unsolder) the instrumented tube lead wires from the amplifier inputs.

12. Using a millivolt potentiometer in EMF output mode, apply reference voltage signals to amplifier input for each channel and record these signals on the FM data recorder. These signals, along with the offset voltage information, allow the overall voltage gain of each channel to be determined. The accuracy of the potentiometer is critical. It should be checked for operational fitness by the electronics service shop before use.

13. Warm bed to next higher temperature and reconnect (solder) leads as before. Repeat steps 8, 9, 10, 11, and 12 for each case of interest.

14. Shut-down the facility as described in Welty (1978). Maintain coolant flow until the bed is cool (less than 395 K).

APPENDIX D

Response Time of the Heat Flux Transducer

The heat flux transducer employed in this study consists of a Micro-Foil Heat Flow Sensor (hereafter referred to as sensor) covered by a 0.127 mm thick stainless steel shim stock. The time constant, for a 63.2% response to a step change in surface heat flux, for the sensor alone, is given by the manufacturer as 0.02 seconds. However, the covering shim stock slows the response greatly.

For purposes of estimating the response time of the combination, it is assumed the response is dominated by the shim stock. This assumption is justified by the value of the time constant obtained. Similar analyses have been carried out by others (Hager, 1965).

Thermal conductivity of the shim stock is much larger than that of the sensor. The temperature difference across the shim stock thickness is neglected. An energy balance for the shim stock is

$$\rho_1 C_1 \delta_1 \frac{dT_w}{dt} = q_1 - h_2 (T_w - T_{w2})$$

where

$$h_2 = \frac{1}{R_{GAGE}}$$

The heat flux which enters the sensor is

$$q_2 = h_2 (T_w - T_{w2})$$

Solution, for a step change in surface heat flux (q_1), yields

$$T_w - T_{w2} = \frac{q_1}{h_2}\left[1 - \exp\left(-\frac{h_2 t}{\rho_1 C_1 \delta_1}\right)\right]$$

and

$$\frac{q_2}{q_1} = 1 - \exp\left(-\frac{h_2 t}{\rho_1 C_1 \delta_1}\right)$$

The time constant for 63.2% response (t_c) is given by

$$\frac{h_2 t_c}{\rho_1 C_1 \delta_1} = 1$$

$$t_c = \frac{\rho_1 C_1 \delta_1}{h_2} = \rho_1 C_1 \delta_1 R_{GAGE}$$

Using a shim stock thickness $\delta_1 = 0.127$ mm, properties of stainless steel, and $R_{GAGE} = 5.28 \times 10^{-4}\ m^2 \cdot K/W$ (as given by the sensor manufacturer), gives

$$t_c = 0.24 \text{ second}$$

Therefore, the time constant for the sensor and shim stock combination is a factor of 12 larger than for the sensor alone.

It is clear that t_c is too large for the heat flux measurements to be interpreted as instantaneous measurements. Data reduction does not require the value of t_c.

Presence of thermal contact resistance, between sensor and tube wall or sensor and shim stock, will slow the response further. These resistances have not been included in the calculation since the Micro-Foil Heat Flow Sensor manufacturer provides R_{GAGE} accurate to only one significant digit (in U.S. customary units $R_{GAGE} = 0.003$ hr·ft^2 °F/Btu). The additional resistances are certainly much less than the above value.